0270-6474/84/0410-2497$02.00/0

Printed in U.S.A.

The Journal of Neuroscience
Vol. 4, No. 10, pp. 2497-2517
October 1984

MORPHOLOGY, DISTRIBUTION, AND SYNAPTIC RELATIONS OF SOMATOSTATIN- AND NEUROPEPTIDE Y-IMMUNOREACTIVE NEURONS IN RAT AND MONKEY NEOCORTEX[1]

S. H. C. HENDRY,* E. G. JONES,*,[2] AND P. C. EMSON‡

* *James L. O'Leary Division of Experimental Neurology and Neurological Surgery and McDonnell Center for Studies of Higher Brain Function, Washington University School of Medicine, Saint Louis, Missouri 63110 and ‡ MRC Neurochemical Pharmacology Unit, Medical Research Council Centre, Hills Road, Cambridge CB2 2QH, England*

Received January 6, 1984; Revised March 23, 1984; Accepted March 30, 1984

Abstract

Neurons in the monkey and rat cerebral cortex immunoreactive for somatostatin tetradecapeptide (SRIF) and for neuropeptide Y (NPY) were examined in the light and electron microscope. Neurons immunoreactive for either peptide are found in all areas of monkey cortex examined as well as throughout the rat cerebral cortex and in the subcortical white matter of both species. In monkey and rat cortex, SRIF-positive neurons are morphologically very similar to NPY-positive neurons. Of the total population of SRIF-positive and NPY-positive neurons in sensory-motor and parietal cortex of monkeys, a minimum of 24% was immunoreactive for both peptides. Most cell bodies are small (8 to 10 μm in diameter) and are present through the depth of the cortex but are densest in layers II-III, in layer VI, and in the subjacent white matter. From the cell bodies several processes commonly emerge, branch two or three times, become beaded, and extend for long distances through the cortex. The fields formed by these processes vary from cell to cell; therefore, the usual morphological terms bipolar, multipolar, and so on do not adequately characterize the full population of neurons. Virtually every cell, however, has at least one long vertically oriented process, and most processes of white matter cells ascend into the cortex. No processes could be positively identified with the light microscope as axons.

The processes of the peptide-positive neurons form dense plexuses in the cortex. In each area of monkey cortex, SRIF-positive and NPY-positive processes form a superficial plexus in layers I and II and a deep plexus in layer VI. These plexuses vary in density from area to area. All appear to arise from cortical or white matter cells rather than from extrinsic afferents. In some areas such as SI and areas 5 and 7, the superficial plexus extends deeply into layers III and IV; and in area 17, two very prominent middle plexuses occur in layers IIIB through IVB and in the upper one-third of layer V; these are separated by layer IVC, a major zone of thalamic terminations, which contains very few SRIF- or NPY-positive processes. The density of the plexuses is greater for NPY-positive processes than for SRIF-positive processes in all areas. In the rat, the plexuses do not display a strict laminar organization but generally are densest in the supragranular layers (I to III) and decline steadily in the deeper layers.

Most synaptic terminals in area 4 and in SI of monkeys that are immunoreactive for either SRIF or NPY are small (0.5 to 1.0 μm), and the cytoplasmic surfaces of all their contained organelles are labeled as well as the cores of the one or two large dense-core vesicles that can be present. Some of these terminals could not be seen to form synapses even in serial thin sections. Where their synapses could be identified they formed symmetric membrane thickenings and occurred principally onto dendritic spines or onto the shafts of small or medium-sized dendrites. Some SRIF-positive and NPY-positive terminals are larger (2 to 3 μm) and contain numerous labeled, large dense-core vesicles. These terminals form asymmetric synapses on large dendritic shafts arising from large nonpyramidal cells.

Several neuroactive peptides have been identified in the mammalian neocortex (Emson and Lindvall, 1979; Emson and Hunt 1984). Among these are the gut peptides, cholecystokinin octapeptide (CCK) and vasoactive intestinal polypeptide (VIP), and the hypothalamic peptide, somatostatin (SRIF), all of which have been determined by radioimmunoassay to be highly concentrated in the neocortex of several species (Reh-

[1] This work was supported by Grant NS10526 from the National Institutes of Health, by the United States Public Health Service, and by the Washington University McDonnell Center. We thank Ms. Bertha McClure for technical assistance and Dr. Gerald Fischbach and Mr. Theodore Usdin for use of their Nomarski microscope.

[2] To whom correspondence should be addressed, at Department of Anatomy, University of California, Irvine, CA 92717.

feld, 1978; Straus and Yalow, 1978; Larsson and Rehfeld, 1979; Emson et al., 1980, 1981, Beinfeld et al., 1981). The effects of application of many of the neuropeptides on cortical neurons have been examined (e.g., Phillis et al., 1978; Phillis and Kirkpatrick, 1980; Kelly, 1982), but the role of the neuropeptides in the function of the cerebral cortex and the position of peptidergic neurons in the circuitry of the cortex remain to be determined.

Previous immunocytochemical studies have identified cells in the rat cerebral cortex displaying CCK-like (Innis et al., 1979; Lorén et al., 1979; Emson et al., 1980; Emson and Hunt, 1981; McDonald et al., 1982d; Hendry et al., 1983b; Peters et al., 1983), VIP-like (Fuxe et al., 1977; Hökfelt et al., 1982; McDonald et al., 1982a), and SRIF-like immunoreactivity (Bennett-Clarke et al., 1980; Krisch, 1980; Finley et al., 1981; McDonald et al., 1982c). In the cerebral cortex of both rats and humans the SRIF-like immunoreactivity has been co-localized in cells that also display avian pancreatic polypeptide (APP)-like immunoreactivity (Vincent et al., 1982a, b), although this APP immunoreactivity has now been identified tentatively as neuropeptide Y (NPY) immunoreactivity (Tatemoto et al., 1982; Allen et al., 1983).

Each of the immunocytochemical studies has identified the vast majority of peptide-immunoreactive neurons as belonging to one of the two fundamental populations of cortical neurons—the nonpyramidal cells. Nonpyramidal cells are the intrinsic or interneuronal elements of the cortex (Jones, 1975, 1983) made up of several classes identified particularly by stereotyped patterns of axonal ramifications and termination (Ramón y Cajal, 1911; Colonnier, 1966; Valverde, 1971; Szentágothai and Arbib, 1974; Jones, 1975; Somogyi, 1977; Fairén and Valverde, 1980; Peters and Proskauer, 1980; Somogyi and Cowey, 1981). Immunocytochemical studies of the localization of glutamic acid decarboxylase (GAD) have also identified several morphological classes of nonpyramidal cells as GABAergic (Ribak, 1978; Peters et al., 1982; Hendry et al., 1983a; Houser et al., 1983a, b) and, therefore, inhibitory (Krnjević, 1974). Studies of the localization of choline acetyltransferase (ChAT) also establish some nonpyramidal neurons as cholinergic (Houser et al., 1983a).

Studies of cortical physiology have identified both inhibitory and excitatory effects exerted by cortical neurons (e.g., Toyama et al., 1981; Asanuma and Rosén, 1973). It may be assumed that the GABAergic nonpyramidal cells are the major inhibitory cells, but relatively little is known about which classes of cells may be responsible for intracortical excitation. SRIF, when applied to hippocampal (Dodd and Kelly, 1981) or neocortical neurons (Phillis et al., 1978; Ioffe et al., 1978; Phillis and Kirkpatrick, 1980; Dichter and Delfs, 1981; Delfs and Dichter, 1983), produces excitatory effects, suggesting that SRIF-immunoreactive neurons may function as excitatory intrinsic neurons in the cerebral cortex. SRIF has also been reported to produce inhibition (Renaud et al., 1975) and complex effects (Dichter and Delfs, 1981; Delfs and Dichter, 1983) on some cortical neurons. Because of the importance of SRIF neurotransmission in the cerebral cortex we have examined the distribution of SRIF-immunoreactive neurons, their processes, and the synaptic contacts in the cerebral cortex of rats and monkeys. Furthermore, because of the reported colocalization of SRIF-like immunoreactivity with APP (i.e., NPY)-like immunoreactivity in some cortical neurons (Vincent et al., 1982a, b), we have also examined the neurons in rat and monkey cortex immunoreactive for NPY.

Materials and Methods

Five cynomolgus monkeys (*Macaca fascicularis*) and eight Wistar rats of either sex were used in this study. Four monkeys and four rats were normal. The others received intraventricular injections of colchicine (100 μg total in rats and 1400 μg in the monkeys) 24 or 48 hr before death. Three of the normal monkeys, the normal rats, the colchicine-treated monkey, and three of the colchicine-treated rats were perfused with 4% paraformaldehyde in 0.1 M phosphate buffer (pH 7.4); the remainder were perfused with 4% paraformaldehyde and 0.125% glutaraldehyde in the same phosphate buffer. Following short periods of postfixation (30 min to 8 hr) the brains were blocked and sectioned either frozen on a sliding microtome or directly on a Vibratome. Section thickness was routinely 40 μm. The entire rat forebrain was sectioned, but the monkey brains were blocked so that only the pre- and postcentral gyri, the superior and inferior parietal lobules, and the occipital lobe were sectioned. For light microscopic immunocytochemistry, the 40-μm-thick frozen sections were preincubated in 5% normal swine serum (NSS) in 0.1 M phosphate-buffered saline (PBS) containing 0.3% Triton X-100 for 4 hr at 4°C. The sections were then incubated in a solution identical to that to which the primary antiserum had been added. Two different anti-SRIF antisera were purchased from ImmunoNuclear Inc. and Dako, Inc. Both antisera were made in rabbits against the cyclic SRIF tetradecapeptide. SRIF antisera were diluted 1:750, and the sections were incubated overnight at room temperature or at 4°C. Anti-NPY antiserum was produced by immunizing rabbits with synthetic NPY consisting of an amino acid sequence identical to porcine NPY and linked to bovine serum albumin (P. C. Emson, unpublished procedure). For immunocytochemistry, the NPY antiserum was diluted at 1:1500 and the sections were incubated overnight at room temperature or at 4°C. After thorough washing in several changes of 1% NSS and 0.3% Triton X-100 in 0.1 M PBS at 4°C for 4 hr, sections were further incubated at room temperature in an unlabeled swine anti-rabbit antiserum or in horseradish peroxidase (HRP)-labeled swine anti-rabbit antiserum (Dako, Inc.) in 5% NSS and 0.3% Triton X-100 in 0.1 M PBS for 1 to 3 hr. After thorough washing in 0.1 M PBS at room temperature, the sections incubated in unlabeled secondary antiserum were next incubated in rabbit peroxidase-antiperoxidase complex for 1 to 3 hr. They were then thoroughly washed in PBS and both they and the sections incubated in HRP-conjugated secondary antiserum were reacted with 3,3′-diaminobenzidine tetrahydrochloride (DAB; Sigma Chemical Co.; 20 mg/100 ml in phosphate buffer) to which 30 μl of 30% hydrogen peroxide per 100 ml had been added. Prior to the DAB reaction, selected sections were pretreated in 1% cobalt chloride; others were immersed after the DAB reaction in osmium tetroxide (0.1% in 0.1 M phosphate buffer) for 30 sec. All frozen sections were mounted on gelatin-coated slides, dehydrated, cleared, and coverslipped. Selected immunocytochemically processed sections and unreacted sections were stained with 0.1% thionin. Areal and laminar boundaries were determined according to published criteria (Jones et al., 1978, 1979; Lund, 1973).

For electron microscopic immunocytochemistry, the sections cut on the Vibratome were incubated exactly as above except that Triton X-100 was omitted from every step. Following reaction with DAB, small wedges of the section containing stained elements were carefully cut out under a dissecting microscope. These were postfixed in 2% osmium tetroxide in 0.1 M phosphate buffer, dehydrated in ascending concentrations of ethanol, and embedded in Spurr's resin. Thin sections were cut at 60 to 70 nm on a Porter-Blum MT-2B ultramicrotome (Sorvall, Inc.) collected on uncoated 200-mesh or on Formvar-coated 50-mesh or single-slot grids and examined either without further staining or after staining with uranyl acetate and lead citrate in a Zeiss EM-9S electron microscope.

For all immunocytochemical reactions, control sections were incubated in the same manner as above except for the replacement of the primary antiserum with normal rabbit serum at a concentration twice that used for the primary. Other control sections were incubated in primary antiserum previously adsorbed in 2, 5, or 10 nmol/ml of appropriate synthetic peptides. Synthetic peptides tested were NPY, SRIF, VIP, CCK (octapeptide), APP, glucagon, secretin, insulin, growth hormone-releasing hormone, motilin, gastric inhibitory peptide, and met- and leu-enkephalin. These were obtained commercially (Bachem, Inc.) or as gifts from Dr. Margery Beinfeld.

A block including the pre- and postcentral gyri of one monkey was frozen and sectioned at 8 μm on a cryostat. The sections were collected in serial order. Every second section was incubated in NPY-adsorbed, anti-SRIF primary antiserum and the alternate sections were incubated in SRIF-adsorbed, anti-NPY primary antiserum. The distributions of labeled somata and nearby blood vessels in alternating sections were plotted at successively higher magnifications using a camera lucida, and the drawings were superimposed using the outlines of the blood

vessels as guides. Parts of the same neuron labeled by the two antisera were then confirmed at high magnification and photographed in a format that included the adjacent blood vessels.

Results

Selectivity of immunocytochemical staining

Sections processed immunocytochemically with either anti-SRIF or anti-NPY antiserum display numerous intensely stained somata, processes, and fiber plexuses in the cerebral cortex and underlying white matter. Faint nonspecific staining of somata and neuropil is also evident in most cases and remains when normal rabbit serum or preadsorbed primary antisera are substituted. This nonspecific staining could be reduced by adsorption of both the primary and secondary antisera with acetone-extracted brain powder, but when present it served as a useful guide to determining cortical lamination. Preadsorption of anti-SRIF antiserum with synthetic SRIF or of anti-NPY antiserum with synthetic NPY, even at the lowest concentration of peptide used, blocks all staining except for the faint, nonspecific staining. Synthetic SRIF does not block NPY staining and synthetic NPY does not block SRIF staining. Preadsorption of either antiserum with the remaining synthetic peptides produces no effect on staining.

SRIF immunoreactivity

Stained somata and processes. Neurons in rat and monkey cerebral cortex displaying SRIF-like immunoreactivity are present in all cell-rich layers (II through VI) and occasionally in layer I (Figs. 1 and 2). SRIF-positive cells are also present in large numbers in the subcortical white matter of monkeys and, to a lesser extent, in rats. These cells generally lie within a millimeter deep to the cortex and are only rarely found in white matter not overlain by cortex, such as the corpus callosum (e.g., Fig. 9). There is some variability in the density of labeled somata from one area of cortex to another (see below), but SRIF-positive cells are present in all of the areas of monkey cortex examined and throughout the rat cortex, including the prepiriform and entorhinal areas. Within each area the greatest density of SRIF-positive somata is found in a superficial band that occupies layers II and IIIA and in a deep band that includes layer VI and the subjacent white matter, but intervening cells in layers IIIB through V are also found (Fig. 3). In the two major bands there is a tendency for stained cells to occur in clusters of three or more.

Most SRIF-positive neurons in rats and monkeys have round or fusiform cell bodies that vary in size from 8 × 8 μm in diameter to as much as 20 × 10 μm, although most are small. Many somata in rat cortex and virtually all in monkey cortex are homogeneously labeled, while the remainder in the rat contain numerous labeled granules scattered throughout their cytoplasm. Arising from all the homogeneously stained somata are at least two and often three or more processes. These are of variable diameter (1 to 5 μm) at their origins but none can be clearly recognized as an axon. The processes of SRIF-positive cells of both monkey and rat cerebral cortex have no systematic pattern of branching. Based on the initial orientations of their processes, the cells might be divided into bipolar, bitufted, or multipolar forms, but when long lengths of their processes are stained, it is clear they adopt a wide variety of shapes which no single name could cover. Some pyramidal-shaped cell bodies are labeled, but no SRIF-positive cell in rat or monkey cerebral cortex appears to be a pyramidal cell based on the distribution and morphology of its processes.

The only consistent feature of SRIF-positive neurons is that one or more of their processes adopt at some point a vertical orientation. This is particularly common for neurons with somata in layers IIIB through VI. SRIF-positive neurons in the superficial and deep strata also posess vertically ascending and descending processes, as well as horizontally oriented ones, and cells in the subcortical white matter send long ascending branches into layers V vand VI and occasionally into more superficial layers.

The processes of most SRIF-immunoreactive neurons in monkey cerebral cortex are smooth at their origins and divide once or twice before giving rise to thin, regularly beaded processes. The beads are rather small (0.5 to 0.75 μm in diameter), usually flattened, and separated from one another by very thin labeled segments, 1 to 2 μm long. Some beaded branches can extend for considerable distances (0.5 to 1.0 mm), apparently without further branching. Others give off branches at regular intervals and end in a spray of branches.

The SRIF-positive cells in the rat cerebral cortex that show granular instead of homogeneous somal labeling form a large proportion (~40%) of the immunoreactive cells. These cells are clustered in the same layers as the homogeneously labeled neurons but display little staining of processes. Their size and their appearance in counterstained sections indicate that they are neurons and not neuroglial cells.

Areal distribution

The distribution of SRIF immunoreactive neurons varies somewhat from area to area within both rat and monkey cerebral cortex (Fig. 3). In monkeys the greatest density of labeled somata is evident in the parietal cortex (areas 5 and 7) and in the precentral motor cortex (area 4). A much lower density is found in the first somatic sensory cortex (SI; areas 3a, 3b, 1 and 2) and in the primary visual cortex (area 17). In rats there is some tendency for SRIF-positive somata to be more densely distributed in the region of the sensory-motor cortex. In these areas, in addition to superficial and deep bands of cells, there is a further middle band in layers IIIB and IV. The highest numbers are found in the prepiriform and entorhinal areas.

The differences in density of SRIF-positive neurons evident between areas within a single species are far less than the differences evident in a comparison of the two species. The density of SRIF-positive somata within any area and within any layer of the rat cortex far exceeds the greatest density of labeled somata in any area or layer of monkey cerebral cortex. In layers II to IIIA of rat sensory-motor cortex an average density of 28.7/mm^2 of SRIF-positive cells is stained in rats, whereas in monkeys the average density is 3.2/mm^2 in area 4 and 2.7/mm^2 in area 3b.

SRIF-immunoreactive cells in the subcortical white matter

Cells displaying SRIF-like immunoreactivity are present in the white matter subjacent to all cortical areas in both rats and monkeys (Figs. 1 and 2). Similar to the distribution of SRIF-positive cells in the monkey cortex, a great density of labeled cells is present in the white matter of the superior parietal lobule and the precentral gyrus than in that of the postcentral gyrus or occipital lobe. The cell bodies are comparable in size and shape to those in the cortex. A large proportion of cells beneath the monkey cortex have fusiform somata with long axes parallel to the layer VI/white matter border. They give rise to two or three large, beaded processes that extend horizontally for some distance but usually turn and ascend vertically or obliquely into the overlying gray matter. Single processes can occasionally be traced from a cell in the white matter up into layer III. The processes of the cells in the white matter of the monkey differ from those in the cortex in having larger, more irregularly shaped beads that are separated by convoluted segments of various lengths. The relatively few SRIF-positive cells in the white matter beneath the rat cortex resemble much

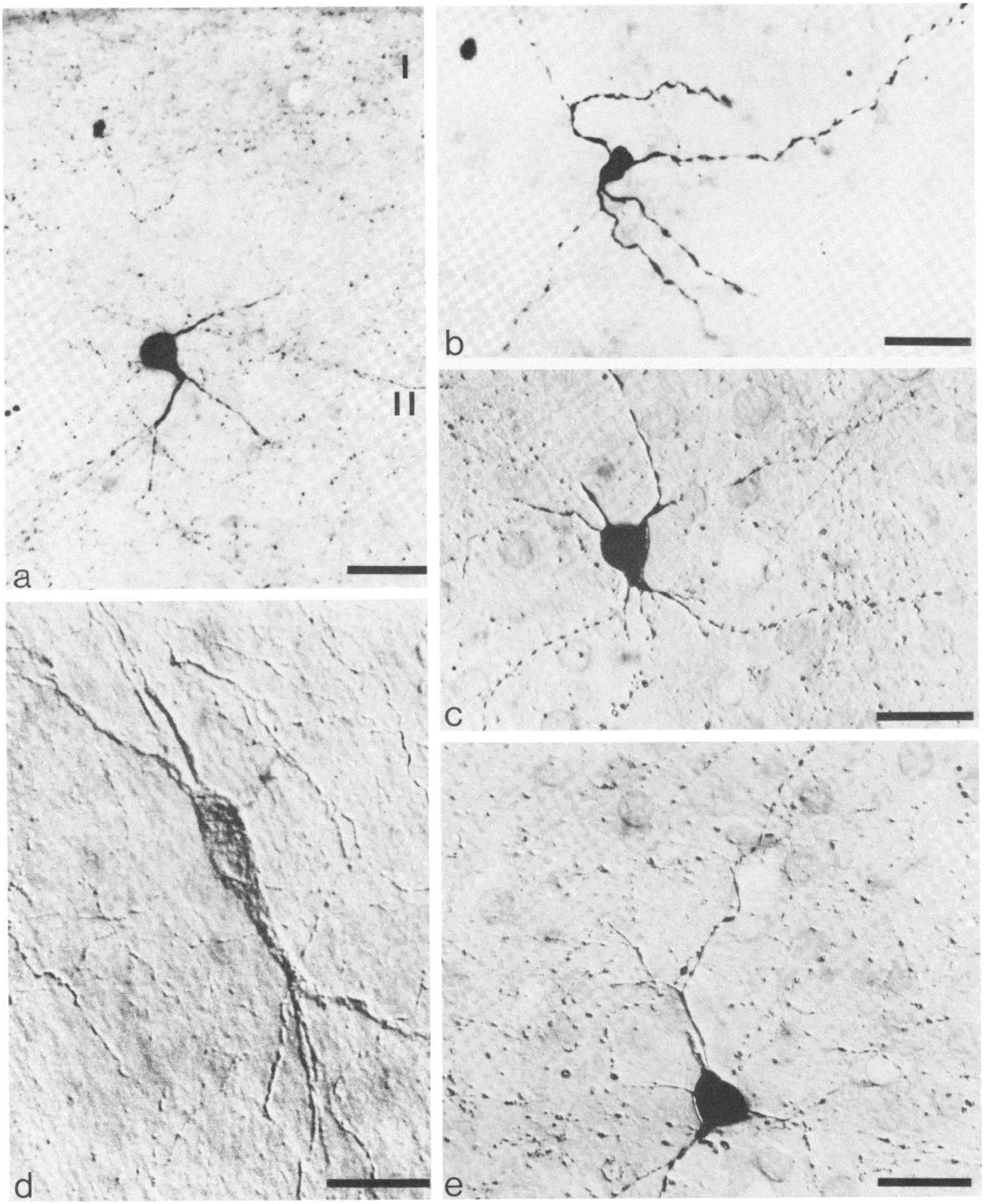

Figure 1. Neurons in rat and monkey cortex displaying SRIF-like immunoreactivity. Processes vary in size but no distinct axons can be identified. *a*, Neuron in layer II of monkey area 4 gives off a large primary process that divides several times into small, beaded branches. SRIF-positive plexus is seen around the cell body and in layer I. *Roman numerals* in this and other figures denote cortical layers. *Bar* = 30 μm. *b*, Cell in the subcortical white matter beneath monkey area 3b with long, coarsely beaded processes. *Bar* = 30 μm. *c*, Nomarski photomicrograph of a neuron in layer III of monkey area 1 giving rise to horizontal and vertically oriented processes. *Bar* = 25 μm. *d*, Nomarski photomicrograph of a neuron in layer V of rat somatic sensory cortex with processes emerging from upper and lower poles. These processes and others around the cell body are not as beaded as SRIF-positive processes in monkey cortex. *Bar* = 25 μm. *e*, Nomarski photomicrograph of a neuron in layer V of monkey area 5 with several thin processes emerging from its soma. Puncta in the neuropil are presumed to be derived from processes of other cells. *Bar* = 25 μm.

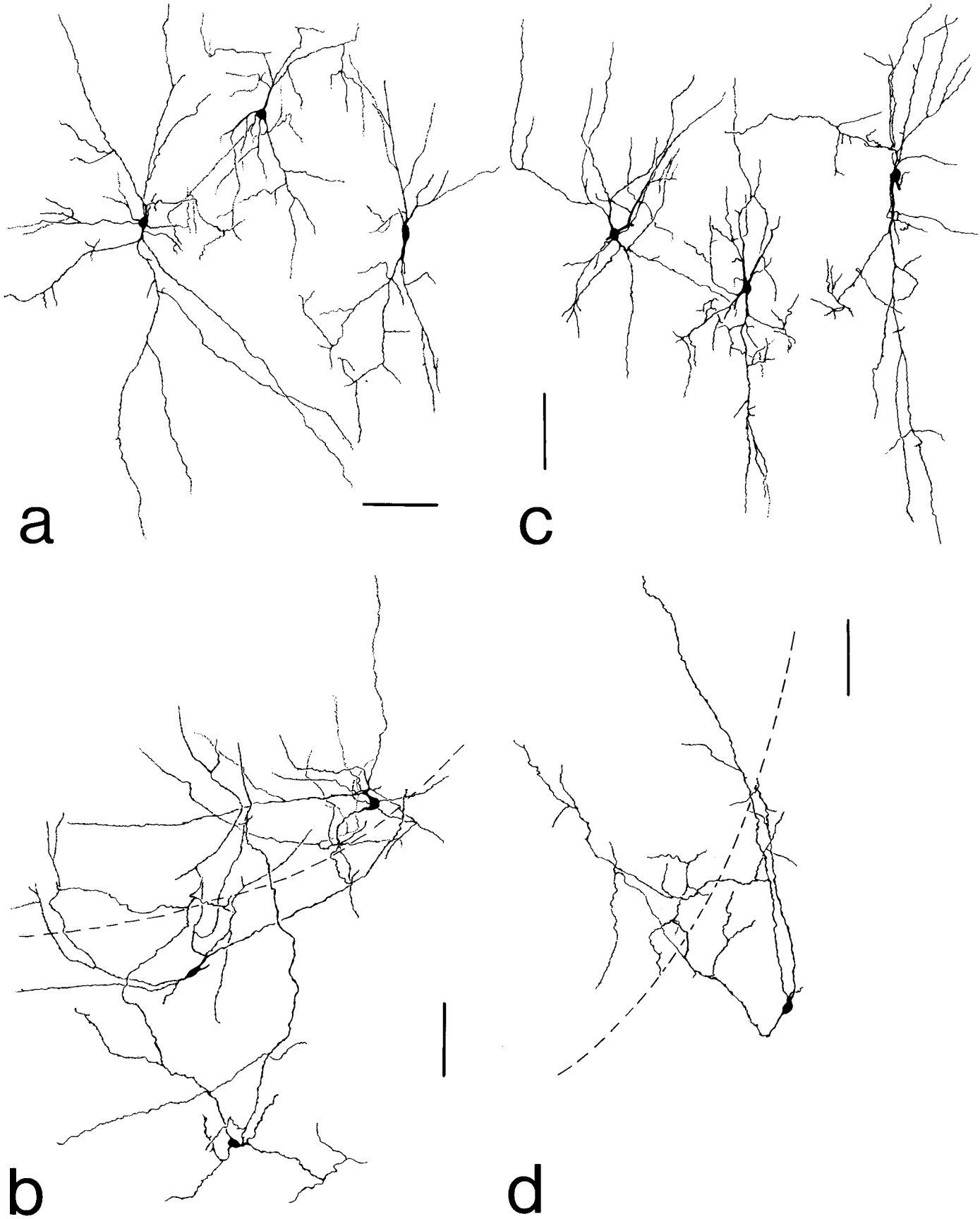

Figure 2. Camera lucida drawings of SRIF (*a* and *b*)- and NPY (*c* and *d*)-immunoreactive cells from various layers and areas of monkey cortex, showing the overall similarities in cell morphology and lack of an identifiable axon. *Bars* represent 100 μm.

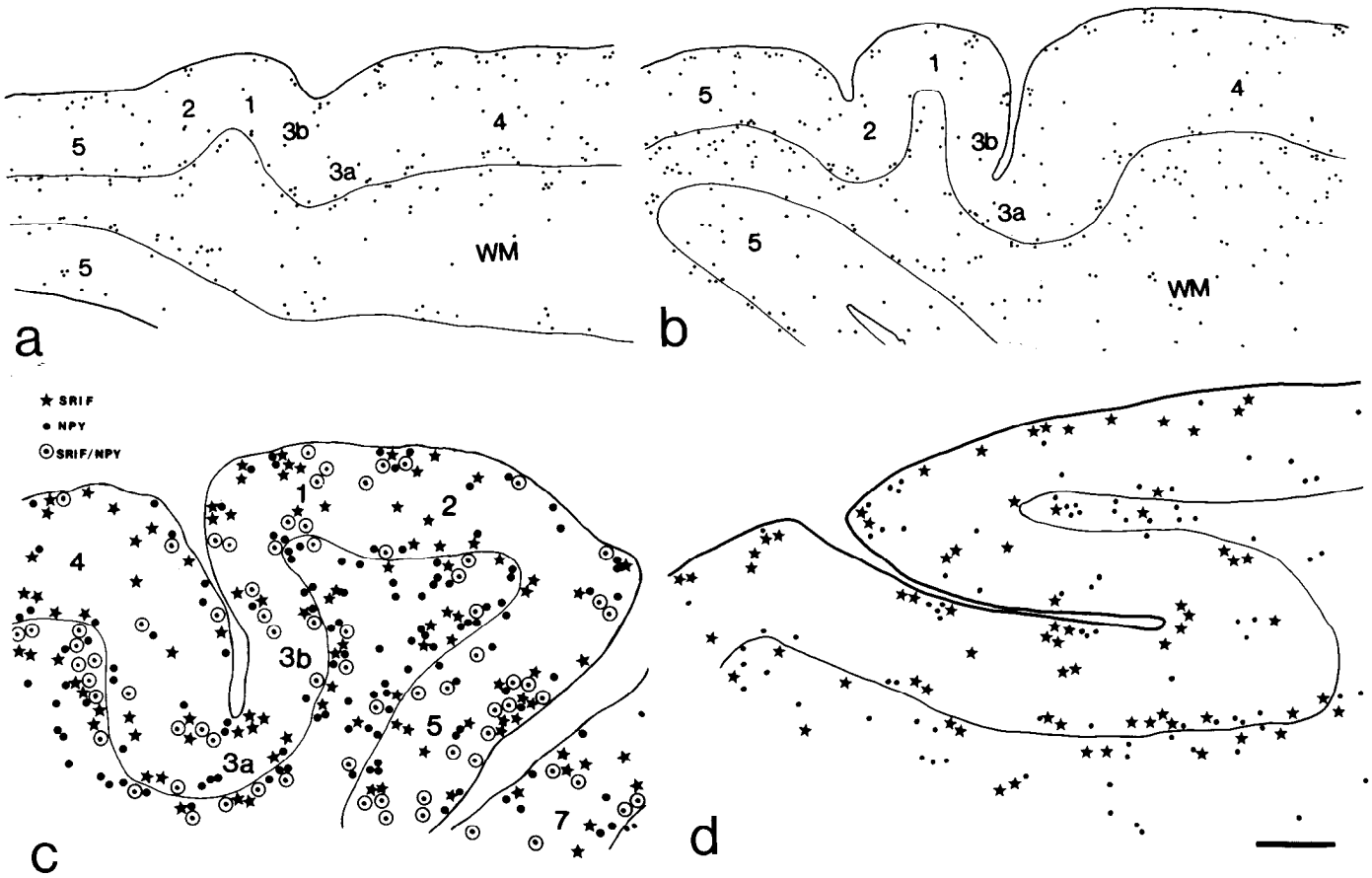

Figure 3. Camera lucida-drawn outlines of sections through the pre- and postcentral gyri (*a* to *c*) and through the occipital cortex (*d*) of monkeys, showing distribution of SRIF-positive (*dots* in *a*, *stars* in *c* and *d*), NPY-positive (*dots* in *b* to *d*), and double-labeled cells (*dots in circles* in *c*). *a* and *b* were drawn from two 40-μ-thick serial sections; *c* and *d* were drawn from six 8-μm-thick sections. See the text for further details. *Bars* represent 1 mm.

more the cells in the cortex than they do their counterparts in the white matter of the monkey.

Intracortical plexuses of SRIF-immunoreactive processes

The many processes of SRIF-positive cells in rat and monkey cerebral cortex form a complicated meshwork that can best be appreciated with darkfield illumination (Figs. 4 to 6). There is a strong tendency for SRIF-positive processes to be radially oriented in the middle layers of the monkey cortex, particularly in area 4. From these arise horizontal and obliquely oriented processes that form two or more plexuses in each area of monkey cortex. All of the SRIF-positive processes appear to arise from cells within the cortex and in the subjacent white matter, and not from fibers of extrinsic origin. However, in each plexus there are many short, twisted SRIF-positive segments and isolated labeled puncta that cannot be traced to their cells of origin.

In the precentral motor area, one plexus occupies the deep part of layer VI and extends just below its junction with the white matter. This plexus is made up of many relatively large vertical and oblique processes originating from cells in the white matter and in layer VI, and those descending from the few immunoreactive cells in layer V. A second plexus is present superficially, in layers I and II, but with its highest density of processes just beneath the pia mater. This plexus arises primarily from cells within layers II and IIIA. Between the superficial and deep plexuses the SRIF-positive processes are much fewer in number and consist mainly of those with a strongly vertical orientation.

Superficial and deep plexuses of SRIF-positive processes, as dense as those in the primary motor area, are present in areas 5 and 7. In addition, a third plexus, continuous with that in the superficial layers, occupies layers IIIB and IV. A similar organization of three loosely organized plexuses is evident in SI, except that each plexus is less dense than in the parietal cortex and the staining is far less dense, overall, than in area 4. This is particularly evident in comparing layer I on the two sides of the central sulcus.

In the primary visual cortex (area 17) of monkeys, a superficial plexus, occupying layers I and II, and a deep plexus in layer VI are again present. Despite a decrease in the density of processes relative to comparable layers in other areas of monkey cortex, it can be seen that there is additional plexus formation in the upper part of layer V and in the deepest part of layer III, in layer IVA, and most of layer IVB. The intervening layer IVC contains few SRIF-positive processes.

Very few vertically oriented processes are evident in any area of rat cerebral cortex. Instead, a moderately thick plexus is present in the layers I to III of most areas. The plexus is made up of short, oblique, twisted segments and isolated puncta that are most numerous beneath the pia mater. In most areas the density of SRIF-positive processes declines progressively below layer III, although an additional deep plexus in layer V or VI exists in some parts of frontal and occiptal cortex.

NPY immunoreactivity

Somata and processes. Neurons in rat and monkey cerebral cortex displaying NPY-like immunoreactivity are similar in

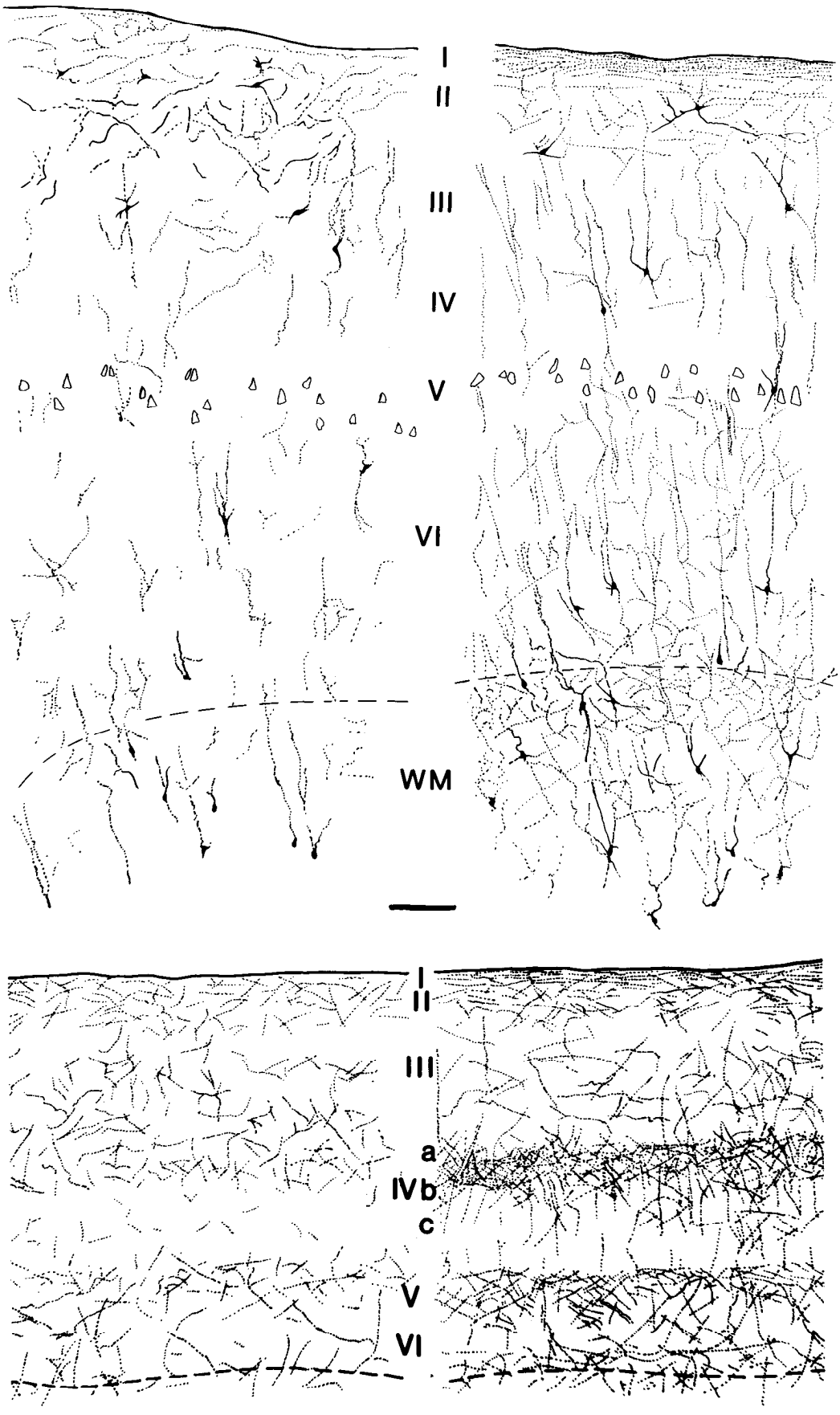

Figure 4. Camera lucida drawing of the major labeled processes and cells made under darkfield conditions from area 4 (*upper*) and area 17 (*lower*) of monkeys. SRIF staining is on the *left*; NPY staining is on the *right*. Note the contribution of vertical cell processes to plexus at different levels and differences in density of SRIF- and NPY-positive processes (cf. Figs. 5 and 6). Layer V is indicated by nonspecific staining of pyramidal cells. *Bars* represent 250 μm.

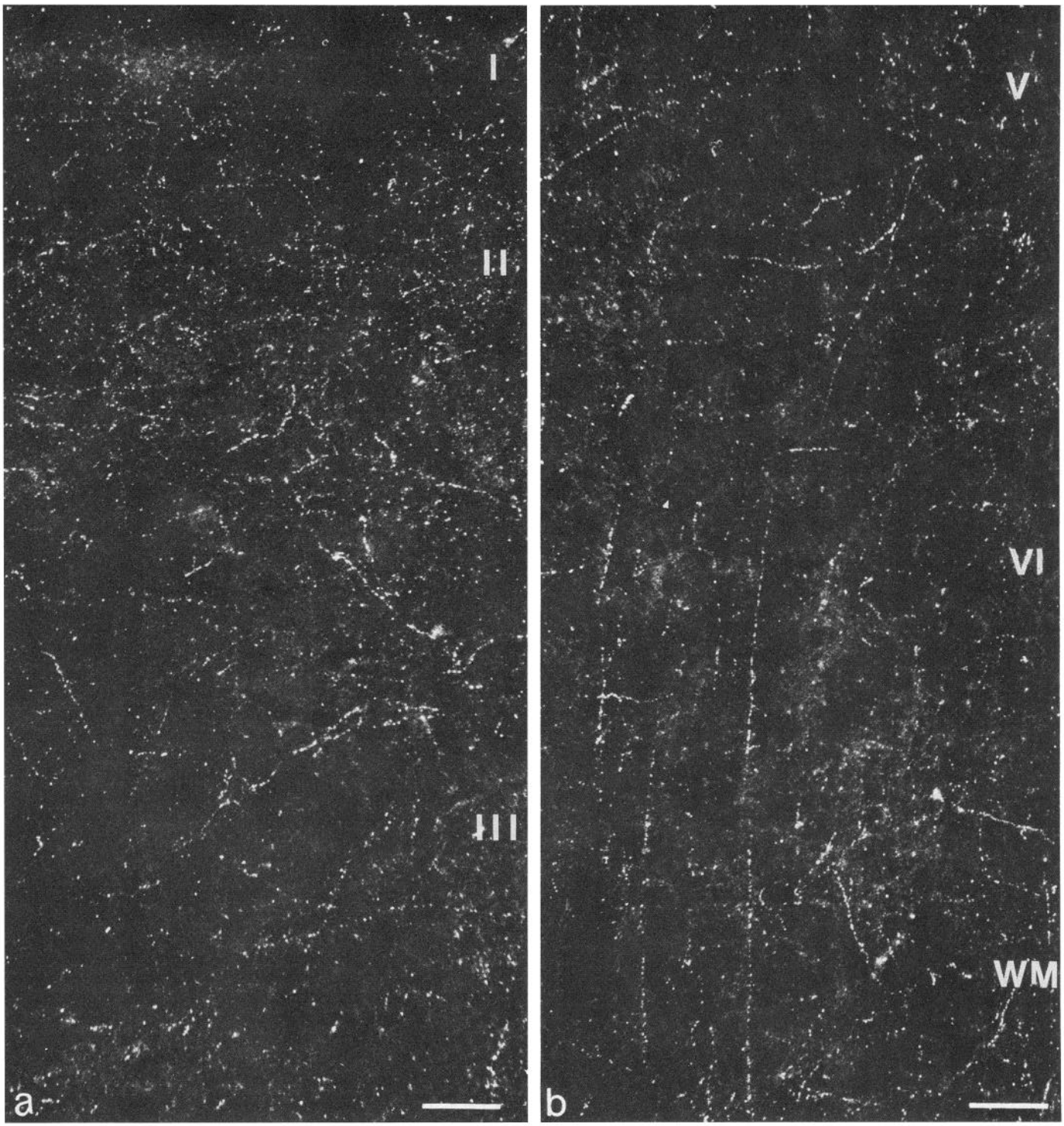

Figure 5. Darkfield photomicrographs of SRIF-immunoreactive processes (*a* and *b*) and NPY-immunoreactive processes (*c* and *d*) in area 4 of monkey cortex. In both sets of micrographs numerous labeled puncta and some horizontally oriented processes are evident in layers I and II

size, morphology, and distribution to SRIF-immunoreactive neurons. Compared with SRIF-positive cells (Figs. 2, 3, and 7 to 9), a smaller number of NPY-positive cells appears to be present in monkey cortex while a greater number is present in the subcortical white matter.

Processes arising from NPY-positive somata, although typically more completely stained than SRIF-positive processes, are also found to emerge at variable angles, to branch extensively, and to produce varied morphological patterns. Like SRIF-positive neurons, NPY-positive neurons in monkeys give off smooth primary processes, 1 to 4 μm in diameter. The smallest may resemble an axon but the largest can break up soon after its origin into fine branches identical to the smallest of primary processes. After one or two divisions, the NPY-positive processes become beaded and remain beaded over the considerable distances (1 to 1.5 mm) that some can be followed. They occasionally divide further, especially at what appears to be their terminal portions, where two or three closely spaced

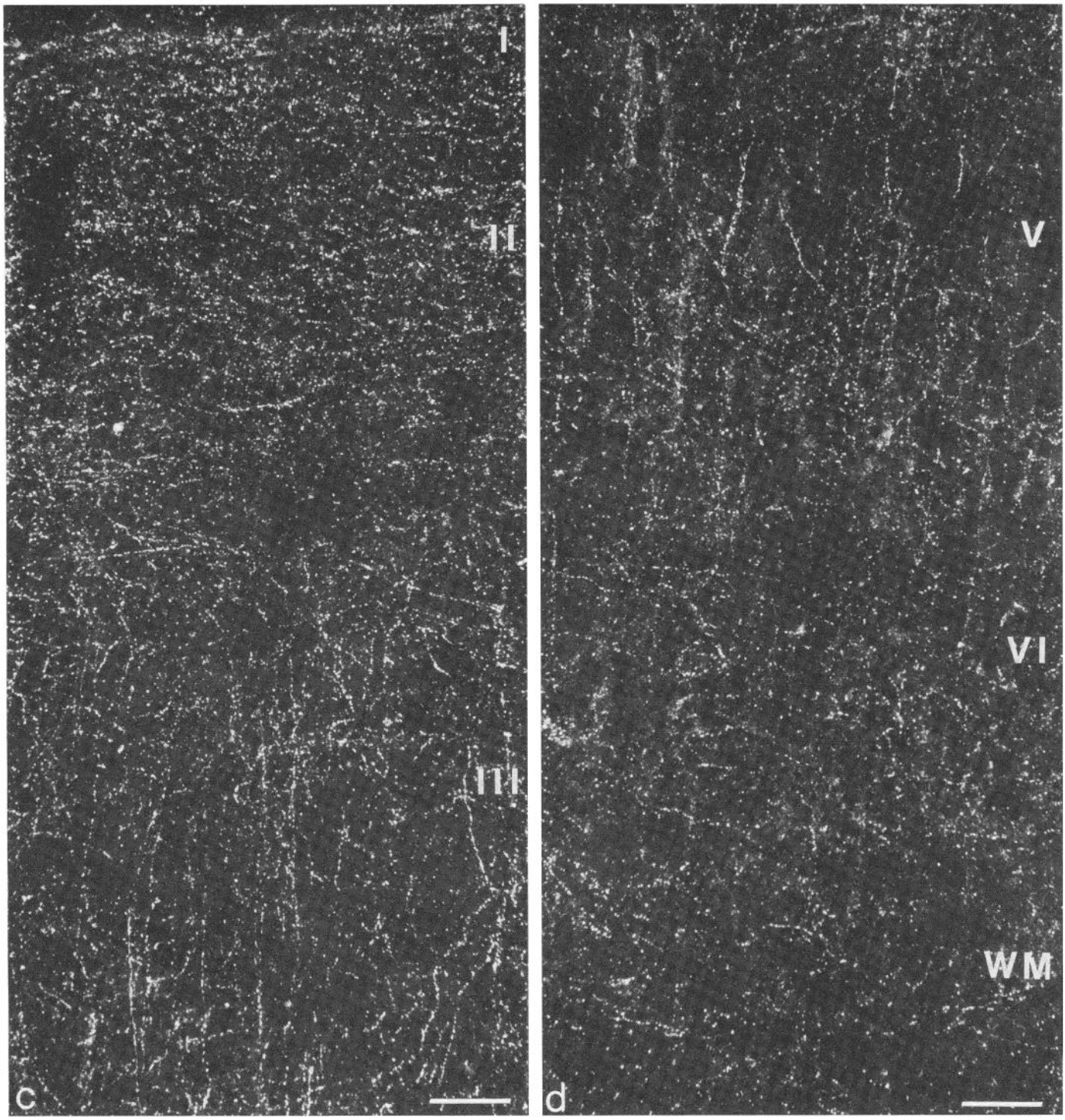

and to a lesser extent at the layer VI/white matter boundary. In between, long vertically and obliquely oriented processes are labeled. The density of labeling for NPY is greater than for SRIF in all layers. *Bars* = 100 μm.

divisions produce a dense tuft of short, finely beaded segments. As in the case of SRIF-positive cells, there is a strong tendency for every NPY-positive cell in monkey cortex to give off one or more vertical processes. However, horizontally oriented processes are also common, as are branches that bend back to form clusters of beaded segments around their parent somata.

The NPY-positive neurons of rat cerebral cortex are homogeneously labeled and do not appear to be as numerous as SRIF-positive neurons. Thus, the contrast in the density of labeled neurons between the two species is not as striking for NPY-positive neurons as it is for SRIF-positive neurons. In the rat cerebral cortex, NPY-positive cells are virtually identical to the homogeneously labeled SRIF-positive neurons in the shapes and sizes of their somata and processes.

Although present in all layers, the greatest density of NPY-positive neurons in monkey cortex is found in a superficial band (layers II and IIIA) and a deep band (layer VI), and as with SRIF-positive neurons, there are apparently more NPY-

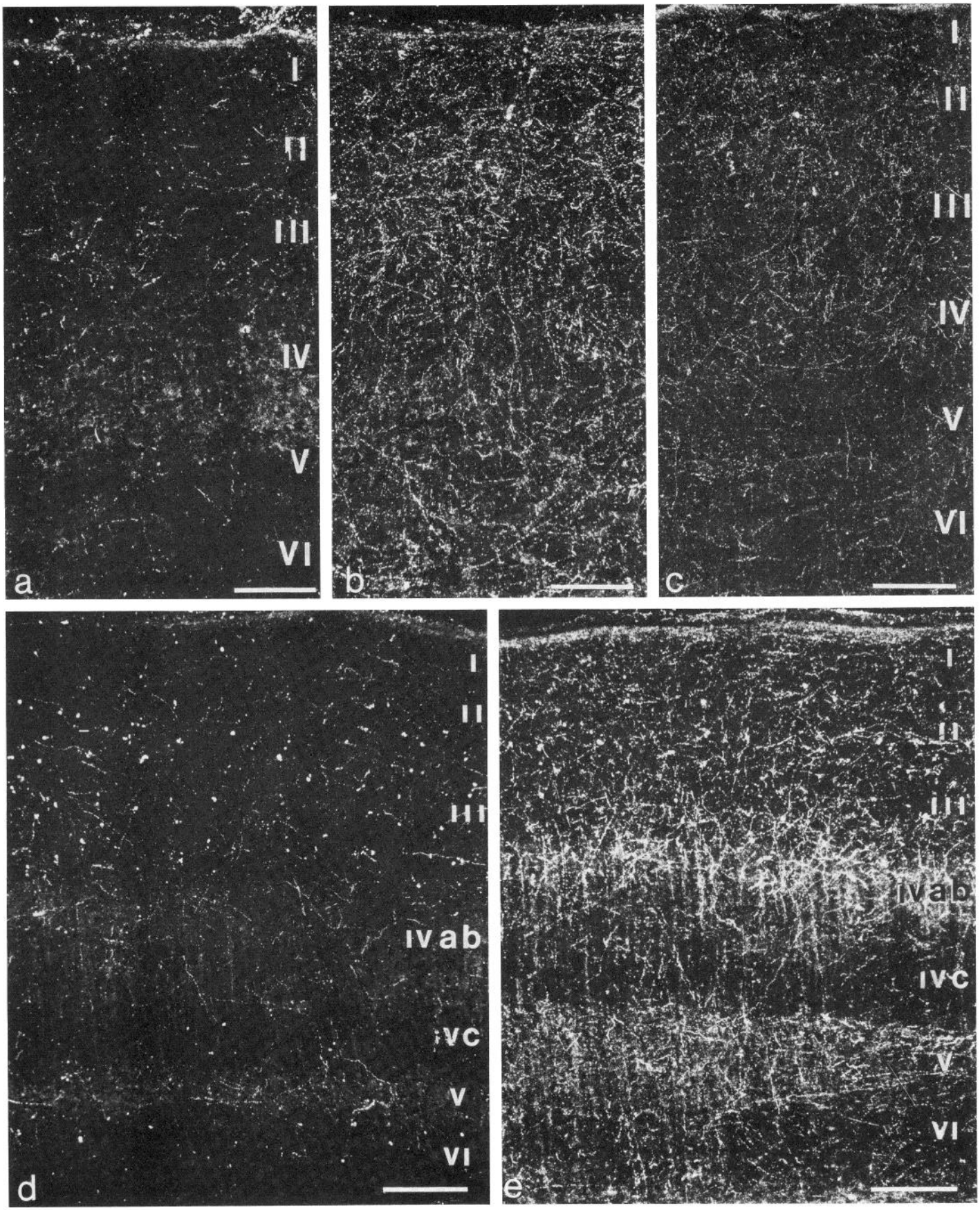

Figure 6. Darkfield photomicrographs of SRIF-immunoreactive processes (*a*, *c*, and *d*) and NPY-immunoreactive processes (*b* and *e*) in monkey cortex. *a* and *b*, Photomicrographs taken from the same region of area 3b showing the relatively light labeling for SRIF (*a*) as compared with NPY (*b*). In area 3b the density of processes in layer I stained for both peptides is lower than the densities in area 4 (cf. Fig. 5), but densities in the middle layers are higher. *Bar* = 200 μm. *c*, Photomicrograph of SRIF-positive processes in area 7 showing greater density than in either

positive cells in certain areas (areas 4, 5, and 7) than in others (SI and area 17). A similar preference for superficial and deep bands is seen for NPY-positive cells in rat cortex, but differences in density among areas are not obvious.

NPY-immunoreactive cells in the subcortical white matter. Many cells displaying NPY-like immunoreactivity are present in the white matter underlying the monkey cerebral cortex (Figs. 9 and 10). The cell bodies and processes are identical in size and shape to those of SRIF-positive cells in the subcortical white matter of the monkey. A greater number of white matter cells display NPY-like immunoreactivity, however, particularly at points 1 mm or more from layer VI. These cells are most numerous in the white matter of the superior parietal lobule. The processes of the NPY-positive white matter cells are very

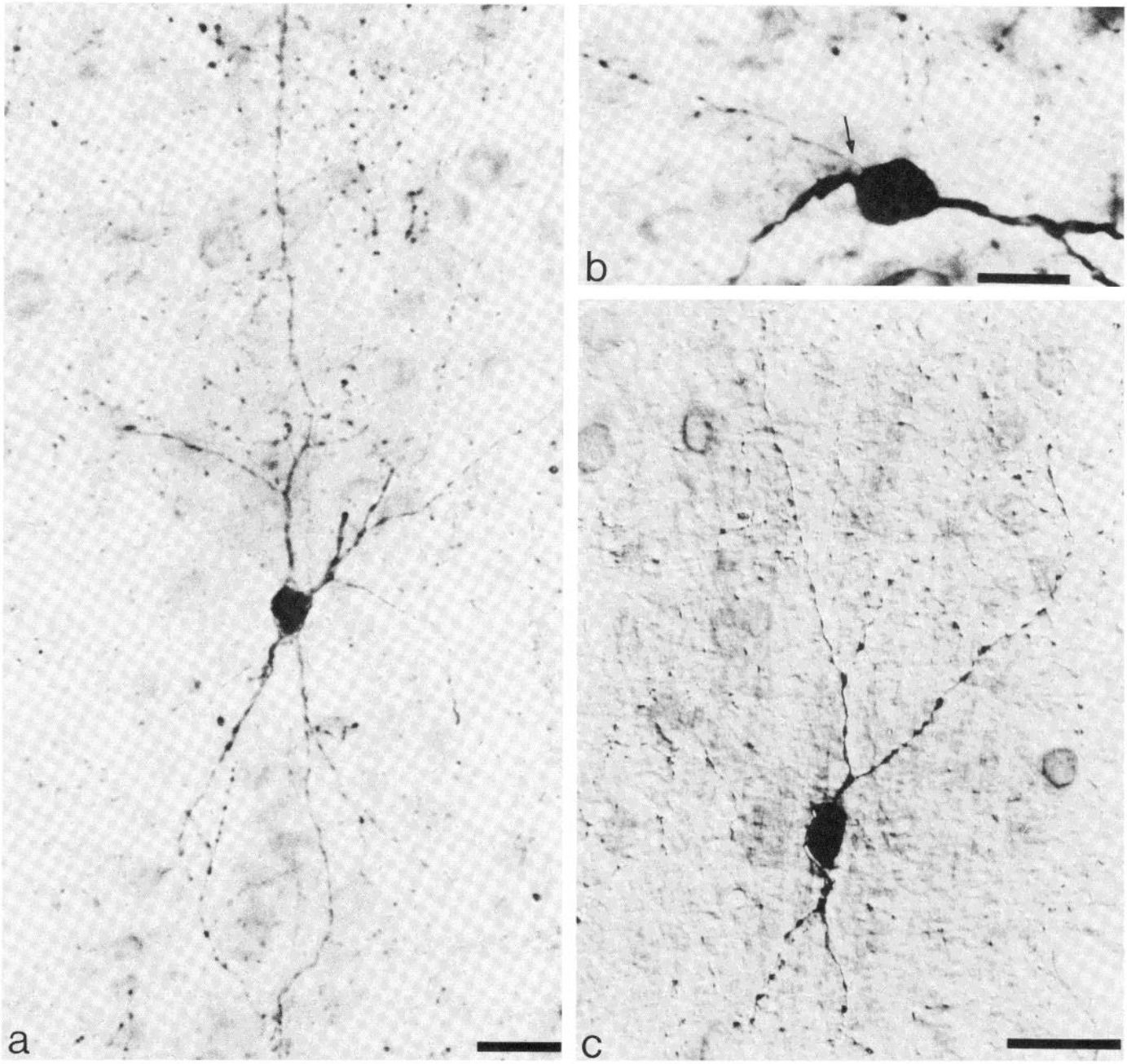

Figure 7. Neurons in monkey cortex displaying NPY-like immunoreactivity. *a*, A neuron in layer III of area 4 gives off several processes of variable size that branch and become beaded. Note the vertical orientation of several of the branches. *Bar* = 25 μm. *b*, A neuron in layer V of area 4 gives off two large primary processes and one very thin process (*arrow*). Although this may be an axon, variability in process size is common and the thicker processes commonly break up into branches identical to the thin one shown here. *Bar* = 10 μm. *c*, Nomarski photomicrograph of a neuron in layer III of area 3b giving rise to vertically ascending and descending beaded processes. *Bar* = 25 μm.

area 4 (Fig. 5*a*) or area 3b (Fig. 6*a*), particularly in the upper and middle layers. *Bar* = 200 μm. *d* and *e*, Photomicrograph of SRIF-positive processes (*d*) and NPY-positive processes (*e*) in area 17 of monkey cortex, from a section through the cortex on the opercular surface (*d*) and from a section through the bank of the calcarine fissure (*e*). Processes immunoreactive for either peptide form two plexuses in layer IIIB-IVB and in layer V. The SRIF-positive and NPY-positive plexuses occupy mainly the upper one-third of layer V but occasionally expand to include most of that layer. Layers IVa and IVb could be distinguished in adjacent counterstained sections but show no difference in the densities of labeling and thus are designated *IVab* in these micrographs. Layer IVc has the lowest density of stained processes. *Bar* = 200 μm.

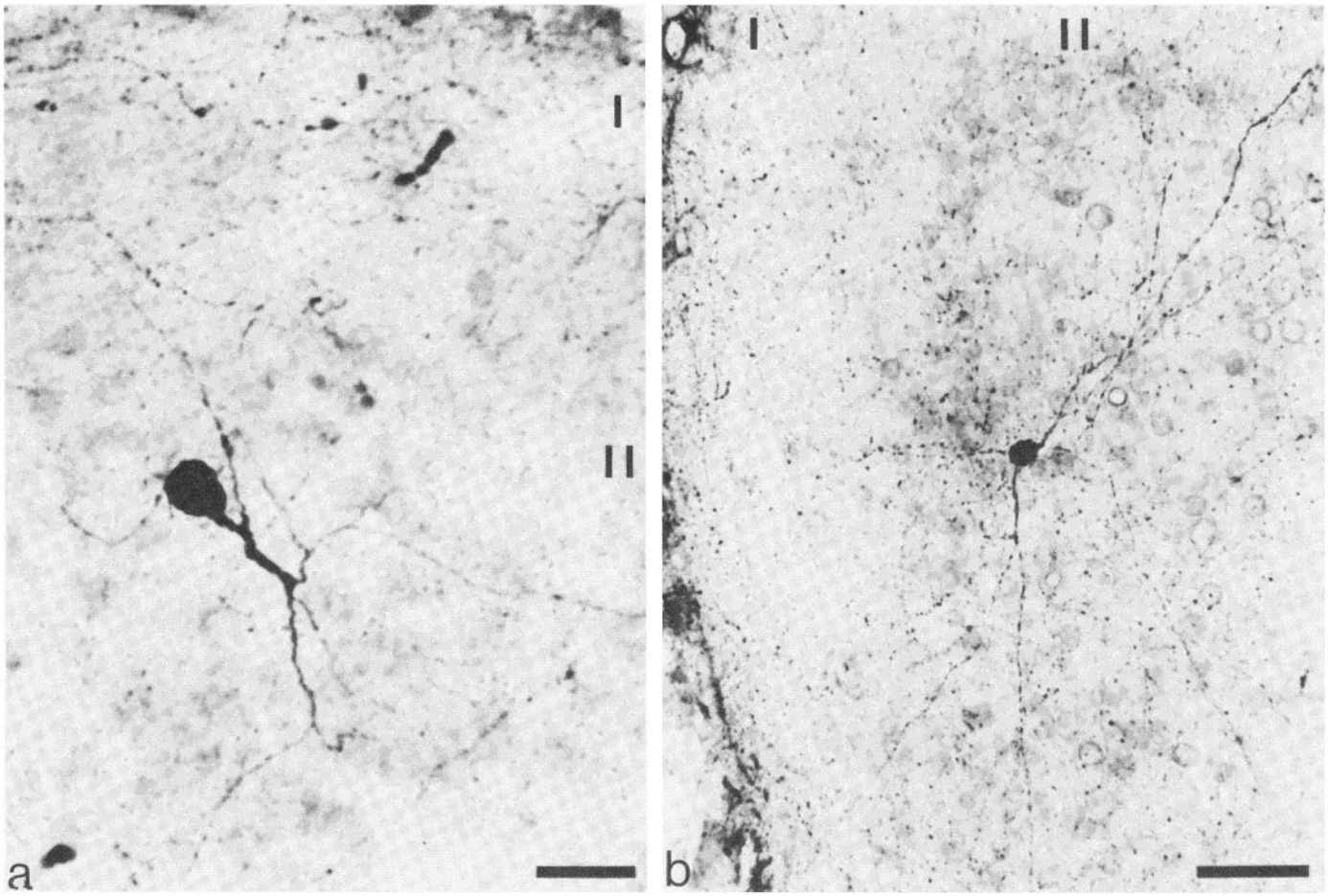

Figure 8. Neurons in the superficial layers of rat (*a*) and monkey (*b*) cortex displaying NPY-like immunoreactivity. *a*, A cell body in layer II of rat parietal cortex from which a large primary process originates and divides into numerous beaded branches, several of which ascend into layer I. *Bar* = 25 μm. *b*, A neuron in the posterior bank of the central sulcus (area 3b) of monkey cortex. The pial surface is to the *left*. Several processes arise from the cell body and extend for considerable distances in all directions and contribute to the layer I-II plexus. Bar = 50 μm.

well stained—they exhibit the same irregular beading and tortuous bending seen in comparable SRIF-positive cells. Most adopt a vertically or obliquely ascending course and enter the overlying cortex after branching close to their parent somata. Some further branching can be seen in layer VI and occasionally layer V, but most processes of these cells ascend through layer IV to layer III, and some have even been traced into layer II without branching.

Plexuses of NPY-immunoreactive processes. The greater number of processes stained for NPY-like immunoreactivity and the greater length of individual stained processes results in plexuses in monkey cerebral cortex that are much denser than plexuses of SRIF-positive processes (Figs. 4 to 6). However, NPY-positive plexuses in monkey cortex have a laminar distribution similar to that of SRIF-positive plexuses and a similar relative density from area to area. In the precentral motor area, superficial (layers I and II) and deep (layer VI/white matter junction) plexuses are separated by large numbers of radially oriented NPY-positive processes. Both SI and the parietal cortex possess a concentration of processes in the middle layers in addition to the superficial and deep plexuses. The large number of NPY-positive processes clearly reveals the rather tight laminar organization of the plexuses in monkey primary visual cortex (Fig. 6*e*). As is the case for SRIF-like immunoreactivity, two relatively minor plexuses of NPY-positive processes are present in layer VI and in layers I and II. However, two middle plexuses similar to those seen with SRIF immunocytochemistry, bracketing layer IVC, are more richly stained for NPY-like immunoreactivity. The lower plexus in layer V is made up of horizontal and oblique processes, many of which appear to arise from cells in layer VI and the subcortical white matter. They are interspersed with long, radially ascending processes, a few of which pass through layer V and almost invariably end in layer IVCβ. The upper plexus again occupies the deepest part of layer III, layer IVA, and most of layer IVB. In this plexus closely spaced bundles of radial processes mix with short twisted segments and thin horizontal processes. The radial bundles make up a system of processes running from the supragranular layers through layer IVB with some entering layer IVCα. In virtually every case they terminate at or near the border of layers IVCα and IVCβ. Thus the two middle plexuses of NPY-positive processes in primary visual cortex are separated by a band within layer IVC that contains relatively small numbers of radial processes derived from deep and superficial cells and meeting in the middle of layer IVC without intermingling.

The plexuses of NPY-positive processes in rat cerebral cortex closely resemble those formed by SRIF-positive processes. Despite the smaller number of NPY-positive cell bodies stained in the rat, the plexuses formed by processes of NPY- and SRIF-positive neurons are of equal density, are preferentially distributed in the supragranular layers, and are frequently made up of large, tight tangles of processes.

Coexistence of SRIF- and NPY-like immunoreactivity in mon-

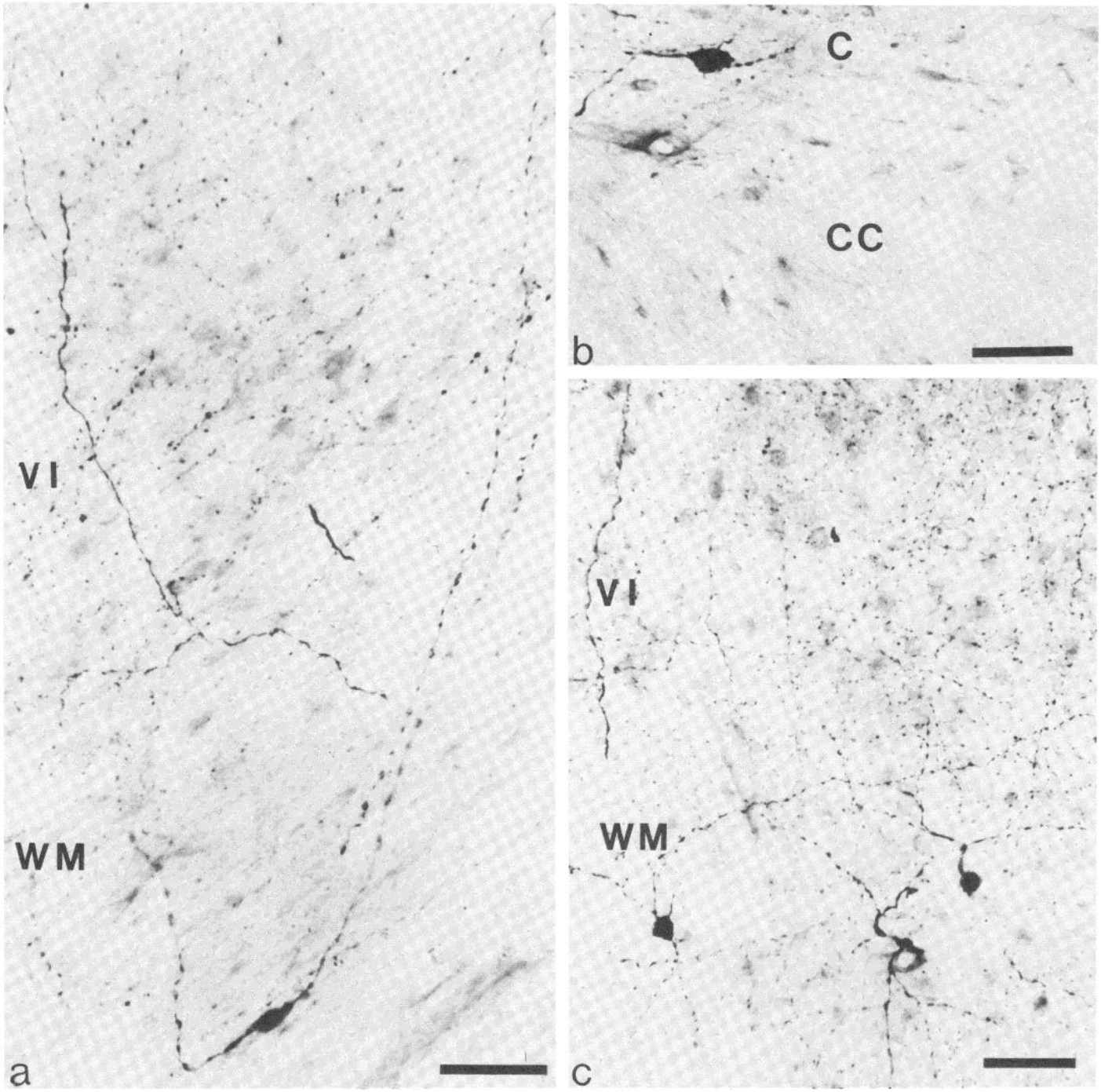

Figure 9. Cells in subcortical white matter of monkeys displaying NPY-like immunoreactivity. *a*, A cell in white matter (*WM*) beneath area 3b gives off coarsely beaded processes that ascend into layer VI. Ascending processes of other white matter cells are also present. *b*, The junction of the subcortical white matter beneath the cingulate cortex (*C*) and the corpus callosum (*CC*). A cell body and several processes are present in the subcortical white matter, but none are evident in the corpus callosum. *c*, Cells in the white matter beneath area 4 give off numerous processes to form a plexus at the junction with layer VI. *Bars* = 50 μm.

key cortical neurons. The possibility that some neurons in monkey cerebral cortex or subcortical white matter display both SRIF-like and NPY-like immunoreactivity was examined by incubating adjacent 8-μm-thick sections in each antiserum. Incubations were done in anti-NPY adsorbed with 10 nmol/μl of synthetic cyclic SRIF and in anti-SRIF adsorbed with 10 nmol/μl of synthetic NPY. The experiment is able to determine the minimum number of stained neurons immunoreactive for both peptides. (Only a neuron sectioned so that part of its soma was contained in two adjacent sections stained with different antisera was judged to colocalize the two peptides for the purpose of quantification). Figure 3 illustrates the results of this experiment. The figure was made by plotting all SRIF-positive and NPY-positive neurons from four alternating sections (numbers 2 through 5) from a series of six through the pre- and postcentral gyri. Sections 2, 4, and 6 were incubated with anti-SRIF, and sections 1, 3, and 5 were incubated with anti-NPY. Double-labeled cells were identified in sections 1

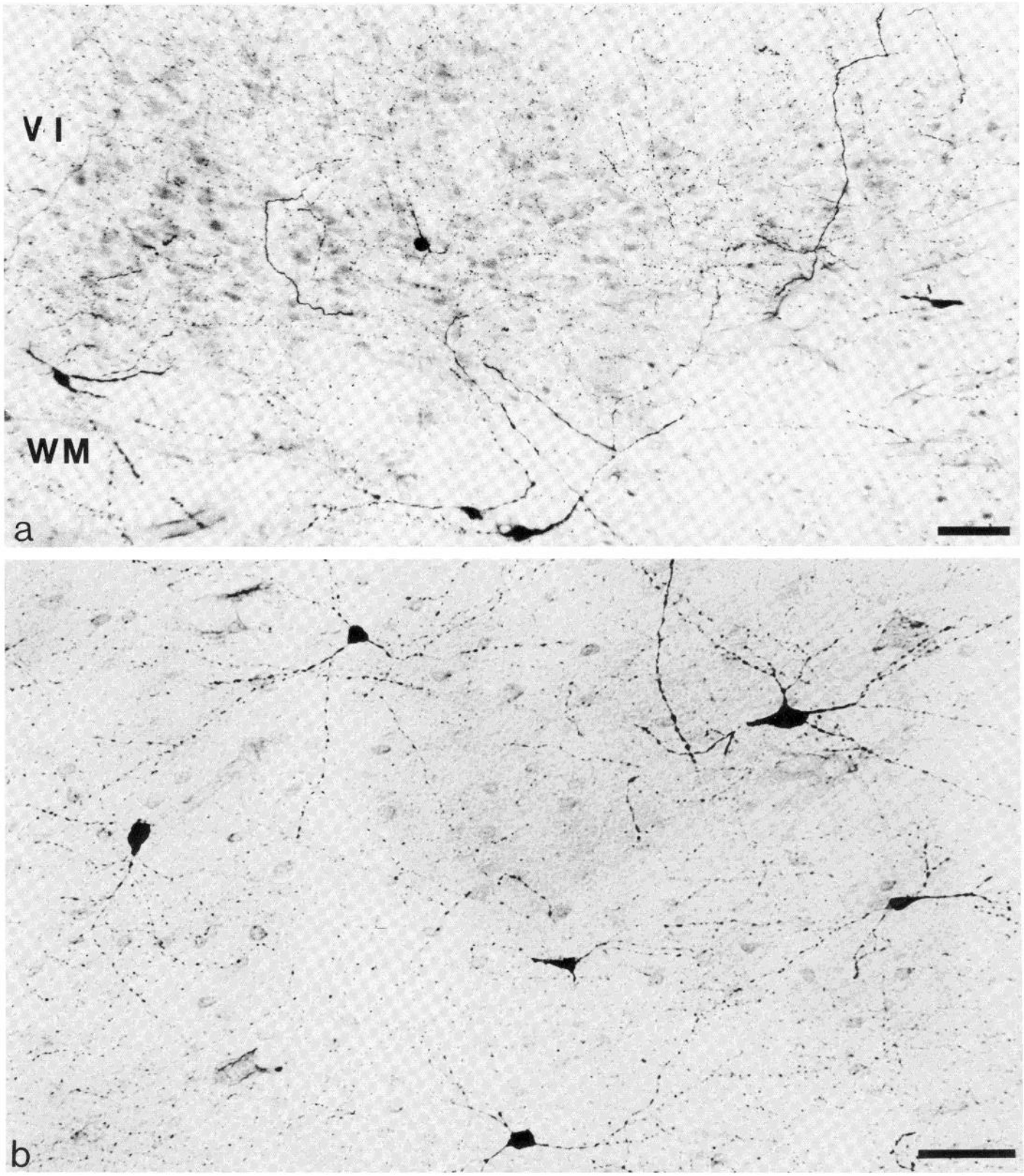

Figure 10. Cells in the subcortical white matter beneath area 5 of monkey cortex displaying NPY-like immunoreactivity. *a*, Cells deep to layer VI give off large numbers of processes that ascend vertically or obliquely into the cortex. *b*, Tangential cut through the white matter. Numerous NPY-positive cells are present. Beaded processes have no apparent preferred orientation. *Bars* = 50 μm.

through 6, photographed (Fig. 11), and also plotted. In the equivalent of these 32 μm of monkey cerebral cortex and subjacent white matter, 176 SRIF-immunoreactive (128 in cortex, 48 in white matter) and 198 NPY-immunoreactive neurons (115 in cortex, 83 in white matter) were detected. Of these, 73 somata are immunoreactive for both peptides, indicating that a minimum of 41% of SRIF-positive cells, 37% of NPY-positive cells, and 24% of all stained cells in the precentral motor area,

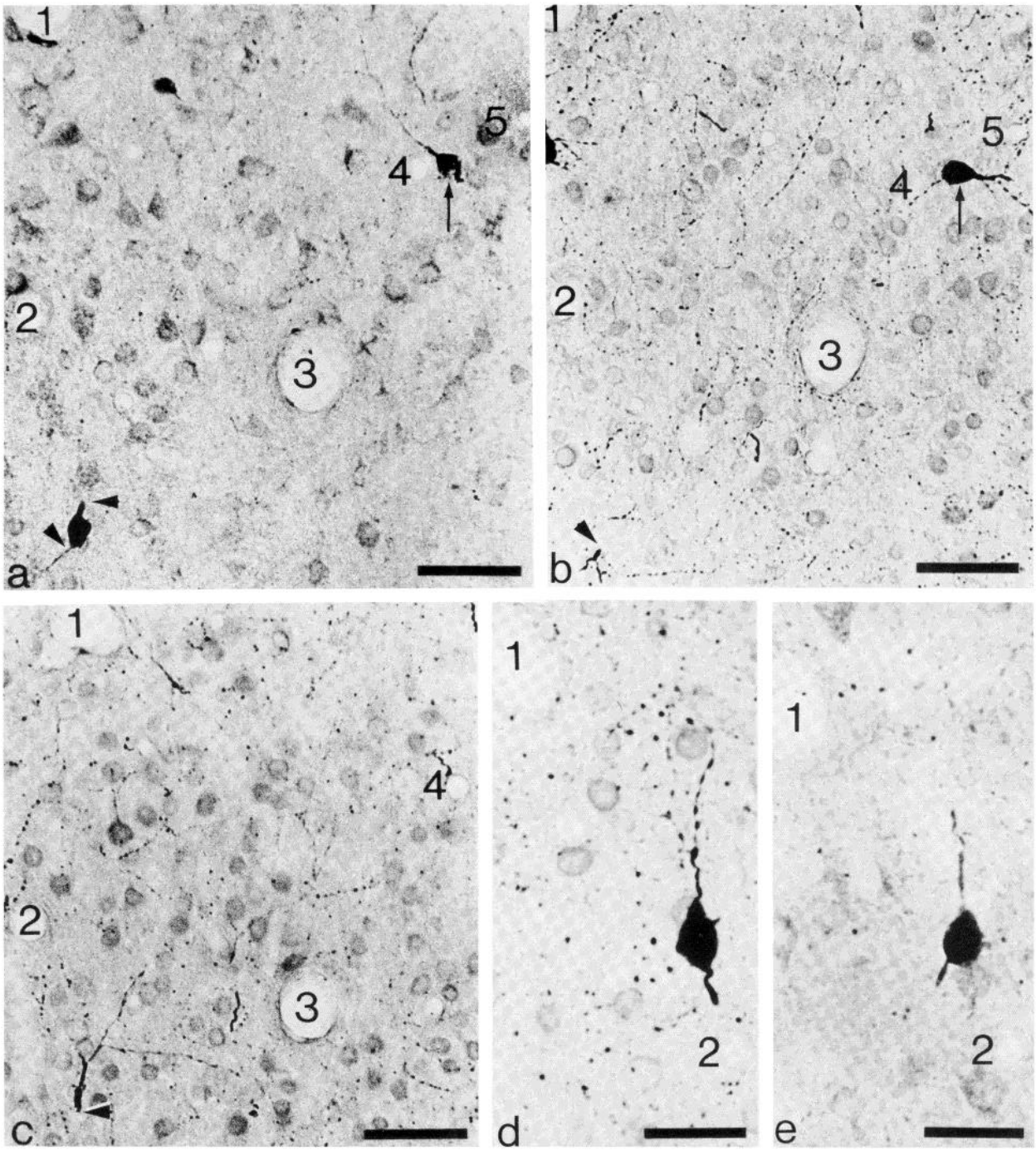

Figure 11. Demonstration of neurons in monkey cortex immunoreactive for both SRIF and NPY. *a* to *c*, Neurons in layer V of area 5. *a*, An 8-μm section processed for SRIF. *b* and *c*, Sections on either side of *a* processed for NPY. The same blood vessels, numbered *1* through 5, are indicated in each micrograph. *Arrows* in *a* and *b* point to the same cell body labeled in each section. An SRIF-positive neuron in the *lower left corner* of *a* gives off two processes that are apparently cut off in this section (*arrowheads*). In *b* and *c* processes of the same size, position, and orientation are seen in adjacent sections (*arrowheads*) Although it is probable that both cells indicated in *a* to *c* are double labeled, only that at the *upper right* was counted since the cell body at *lower left* was not cut in both sections. *Bars* = 25 μm. *d* and *e*, A neuron in layer III of area 4 immunoreactive for NPY (*d*) and SRIF (*e*). The same blood vessels are numbered *1* and 2. Bars = 15 μm.

SI, and areas 5 and 7 of monkeys are positive for both peptides. Similar analysis with other series of sections reveals similar percentages of double-labeled cells. There appears to be little difference between the cortical areas in the percentage of double-labeled cells and, as would be expected from the laminar distribution of cells immunoreactive for either peptide alone, most cells immunoreactive for both are present in the supragranular layers, in layer VI, and in the white matter. However, double-labeled cells are clearly present in the middle layers as well.

The morphology of cortical neurons in which SRIF and NPY appear to be colocalized is the same as described for either population of peptide-positive neurons. The same variability of form with a tendency to give off beaded vertical processes is evident. On many occasions processes stained for SRIF could be followed into an adjacent section where they were found also

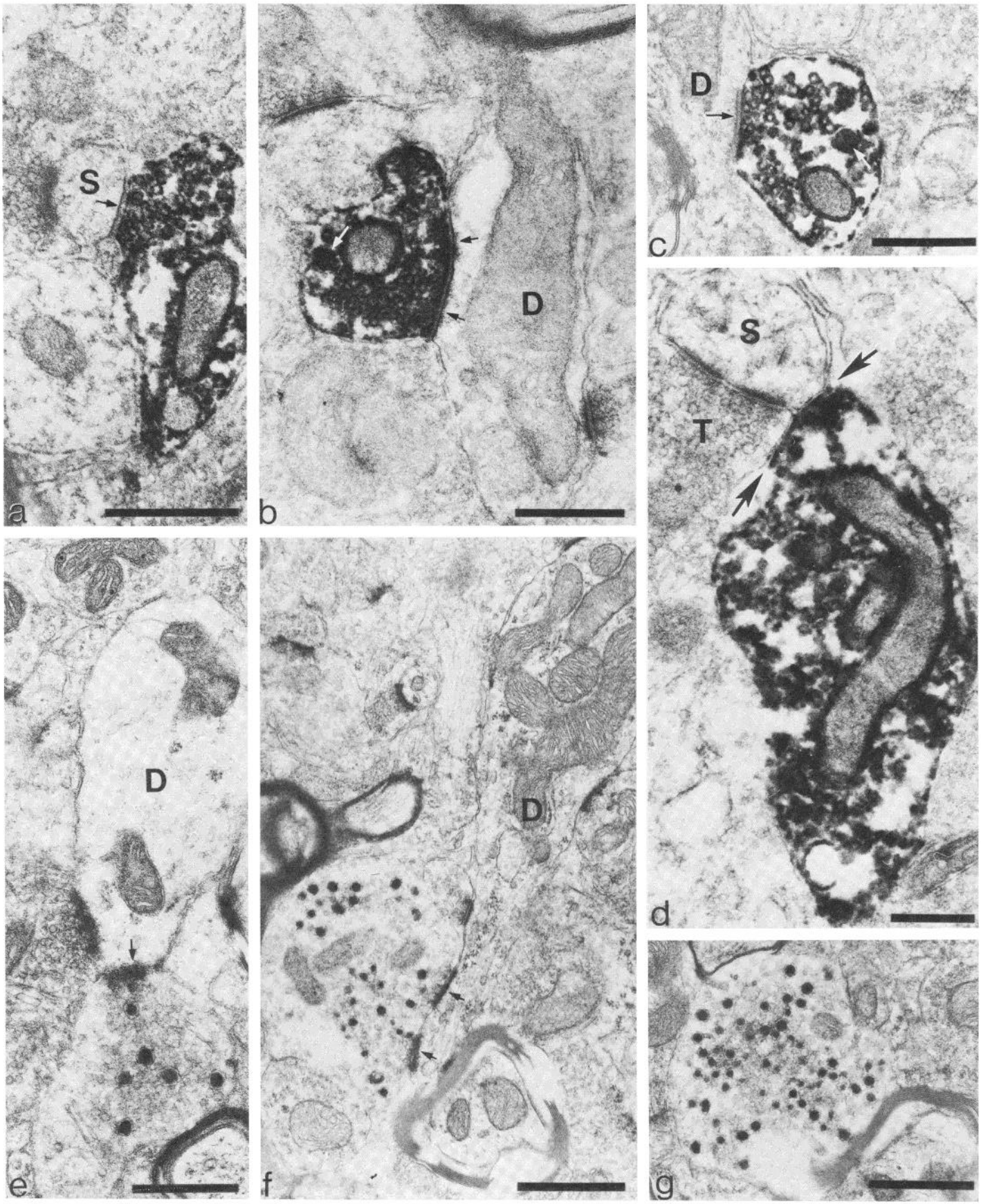

Figure 12. Electron micrographs of terminals in monkey cortex displaying SRIF-like (*a*, *c*, and *e*) and NPY-like (*b*, *d*, *f* and *g*) immunoreactivity. *a*, An SRIF-positive terminal in layer III of area 4 forms a symmetric synapse (*arrow*) onto a spine (*S*). Reaction product is distributed along the surfaces of mitochondria and small synaptic vesicles. *Bar* = 0.5 μm. *b* and *c*, NPY-positive (*b*) and SRIF-positive (*c*) terminals forming

to be NPY positive (Fig. 11). Therefore, the percentage of cells immunoreactive for both peptides is probably greater than that obtained from quantifying double-labeled somata alone.

Electron microscopy of peptide-positive terminals

Many vesicle-filled profiles displaying SRIF- or NPY-like immunoreactivity are found in monkey SI and precentral motor cortex (Fig. 12). We call these profiles terminals because of their population of clear vesicles the same size as synaptic vesicles, but we have traced none of them to identifiable axons. When these terminals are followed through a series of sections they are found to be swellings between very thin (0.2 to 0.3 μm), smooth segments that may be either dendrites or axons.

Most SRIF- and NPY-positive terminals in each layer are rather homogeneously labeled with dense reaction product scattered throughout the cytoplasm (Fig. 12, *a* to *d*). Reaction product is particularly abundant along the external surfaces of mitochondria and synaptic vesicles. Most vesicles within these terminals are small (40 to 50 nm), clear, and usually round, although occasional large dense-core vesicles (80 to 100 nm) are found that contain reaction product (Fig. 12, *b* and *c*). Within some terminals circular regions approximately the size of large dense-core vesicles exist, but they are devoid of either reaction product or other observable contents.

Many homogeneously labeled SRIF-positive terminals and a smaller proportion of similar NPY-positive terminals form observable synaptic contacts with one of a number of unlabeled postsynaptic elements. In all cases, these terminals form symmetric synaptic contacts (Fig. 12, *a* to *c*). Most SRIF-positive terminals and some NPY-positive terminals appear to contact the shafts of medium-sized dendrites, some of which are radially oriented. We have not yet been able to determine from our examination of serial sections whether these postsynaptic dendrites are smooth or spiny or from what type of neuron they arise. SRIF-positive and NPY-positive terminals also form symmetric synapses onto profiles that are either spines or small dendritic shafts cut in cross-section.

The majority of homogeneously labeled NPY-positive terminals and a smaller proportion of SRIF-positive terminals lie adjacent to unlabeled profiles of spines, other terminals, dendrites of variable size, and somata, without forming synaptic contacts in single thin sections. Although the membranes separating the labeled terminals and unlabeled profiles are frequently parallel (Fig. 12*d*), membrane thickenings are not evident. Some NPY-positive terminals, serially sectioned throughout their extent, were not found to form synaptic contacts at any point along their lengths. Commonly NPY-positive or SRIF-positive terminals are adjacent to an unlabeled terminal containing small spherical vesicles and to the spine with which this makes an asymmetric synapse (Fig. 12*d*). The membrane of the labeled terminal is parallel to the membranes of both the pre- and postsynaptic elements, but thickenings or other specializations are not apparent.

A small number of NPY- or SRIF-positive terminals are not homogeneously labeled. These terminals are usually large (2 to 3 μm in diameter) and contain many small spherical vesicles as well as several well preserved, large dense-core vesicles (Fig. 12, *e* to *g*). The immunocytochemical reaction product is found only within the large dense-core vesicles; none could be detected in the cytoplasm or along the membranes of mitochondria or small vesicles, even in a small number of terminals examined in serial sections. The synapses formed by these terminals are asymmetric. The terminals synapse principally on large dendritic shafts, including some shafts that receive many other synaptic contacts. One such dendrite receiving an asymmetric synapse from a large NPY-positive terminal could be followed through serial sections to its parent soma, a large nonpyramidal cell in layer V of the precentral motor cortex.

Discussion

The idea that certain peptides may function either as classical neurotransmitters or as other less conventional modulators of neuronal activity has lead to widespread interest in their biosynthesis, cellular localization, and mode of action (for review see Hökfelt et al., 1980). Of the two studied here, SRIF was first isolated as a hypothalamic peptide hormone (Brazeau et al., 1973), but its neuroactivity (e.g., Renaud et al., 1975; Ioffe et al., 1978; Nicoll, 1978; Olpe et al., 1980), its localization (Bennett-Clarke et al., 1980; Finley et al., 1981; McDonald et al., 1982c), the identification of its putative receptors (Srikant and Patel, 1981) in many parts of the central nervous system, and the evidence that it is released from synaptosomes by depolarizing stimuli in a calcium-dependent manner (Iversen et al., 1978; Bennett et al., 1979) indicate it may act as a neurotransmitter. By contrast, NPY was first isolated from porcine brain extracts using a strategy for detecting peptides with a carboxy-terminal alpha-amide (Tatemoto et al., 1982), a characteristic of peptides with biological activity. It is a member of the pancreatic polypeptide family. Although it appears to be widespread in the brain (Allen et al., 1983), little is known about the exact localization of NPY or about its possible effects on neuronal activity. There is substantial evidence to indicate that immunocytochemical localization of APP-like immunoreactivity in the mammalian brain (Lundberg et al., 1980; Hökfelt et al., 1981; McDonald et al., 1982b); Vincent et al., 1982a, b) represents, instead, NPY immunoreactivity (see Allen et al., 1983).

The two antisera to SRIF used in the present study are both directed against the 14-amino acid peptide SRIF-14. A prosomatostatin-related peptide made up of 28 amino acids (SRIF-28) has been isolated from rat brain, and since it includes SRIF-14 at its C-terminus (Benoit et al., 1982), SRIF immunoreactivity seen in the present study, particularly in somata (Morrison et al., 1983), may also represent the larger peptide. Staining of fine neuronal processes in rat neocortex has been reported previously using antisera against another prosomatostatin-related peptide (SRIF-28, 1–12) that includes the 12 N-terminal amino acids of SRIF-28 (Morrison et al., 1983). The staining seen in the present study probably excludes SRIF-28, 1–12 and thus indicates that SRIF-14 or SRIF-28 can also be demonstrated in fine processes of rat and monkey neocortex. The localization in monkey cerebral cortex of SRIF-28, 1–12 and of another peptide derived from prosomatostatin (Lechan et al., 1983) is unknown.

In the present study we have been concerned with four primary issues. (*1*) Do cells displaying SRIF-like or NPY-like immunoreactivity belong to a single class? (*2*) What is their distribution in the cortex and how does it vary from area to

symmetric synapses (*black arrows*) onto small dendrites (*D*) in layer V of area 4. The reaction product not only coats the cytoplasmic surfaces of mitochondria and of small spherical vesicles but is also found within large dense-core vesicles (*white arrows*). *Bars* = 0.5 μm. *d*, An NPY-positive terminal in layer III of area 3b. The membranes of the labeled terminal are parallel (*arrows*) to the membranes of a spine (*S*) and an unlabeled terminal (*T*), but no membrane specializations are evident. *Bar* = 0.25 μm. *e*, A terminal in layer III of area 3b from material processed with anti-SRIF, showing immunocytochemical reaction product confined to large dense-core vesicles. The terminal forms an apparently asymmetric synapse (*arrow*) with a dendrite (*D*) *Bar* = 1 μm. *f*, A terminal in layer V of area 4 from material processed with anti-NPY, showing immunocytochemical reaction product confined to large dense-core vesicles. The terminal forms asymmetric synaptic contacts (*arrows*) with a large dendrite (*D*). The dendrite receives numerous synapses from other unlabled terminals. *Bar* = 1.0 μm. *g*, Serial section of *f* showing the labeled terminal in a more superficial part of the block. A greater number of large dense-core vesicles are labeled. *Bar* = 1.0 μm.

area and within an area? (*3*) What are their synaptic relationships? (*4*) Are the two peptides colocalized?

The present study indicates that all cells containing one or both peptides are nonpyramidal in form and can thus be considered intrinsic or local circuit, cortical neurons (Jones, 1975, 1983). We could detect no evidence of afferent or efferent fibers containing the peptides. Other workers, studying the localization of SRIF or APP immunoreactivity, have also reported their localization in nonpyramidal cells of the rat (Finley et al., 1981; McDonald et al., 1982b, c; Vincent et al., 1982b) or human (Sorenson, 1982; Vincent et al., 1982a) cortex. Two other peptides, CCK and VIP, have also been localized in cortical nonpyramidal cells of rats (e.g., Innis et al., 1979; Emson et al., 1980; McDonald et al., 1982a, d) and primates (Hendry et al., 1983b), and it appears that this is also true of the localization of enzyme markers for the presence of the transmitters acetylcholine and aspartic acid (Altschuler et al., 1983; Houser et al., 1983a).

We consider that SRIF-immunoreactive cells and NPY-immunoreactive cells form a relatively homogeneous class of small, nonspiny, nonpyramidal neurons whose individuality cannot be expressed in the conventional terms bipolar, bitufted, multipolar, and so on. Some workers might prefer to regard the cells as belonging to several morphological types that can be specified by these names. We think it more important, however, to focus on the features that the cells have in common. Virtually all have small cell bodies and long beaded processes that have a strong tendency to become vertically oriented and to form plexuses of fine beaded branches in certain layers. In neither population of peptide-immunoreactive cells were clearly distinguishable axons seen in light microscopic preparations.

Neurons immunoreactive for SRIF, CCK, VIP, or APP have been referred to as bipolar, bitufted, or multipolar types in previus studies of the rat neocortex (Innis et al., 1979; Lorén et al., 1979; Sims et al., 1980; Finley et al., 1981; McDonald et al., 1982a, b, c, d; Hendry et al., 1983b; Peters et al., 1983). However, variability in the extent of staining of processes and differences in descriptions by different authors of the same immunoreactive cell type are common. This suggests again that the conventional morphological descriptions may not be particularly useful for classifying the peptide containing cortical neurons. Although it seems evident from our results that many SRIF-immunoreactive cells are also NPY immunoreactive, it is not known whether these cells also contain VIP or CCK. The differential distribution of VIP- and CCK-immunoreactive cells in comparison with SRIF- and NPY-immunoreactive cells would suggest that this is not the case. On the other hand, the overall similarity in the morphology of the cortical peptide neurons raises the issue of such multiple colocalization in at least some of them.

Neurons immunoreactive for ChAT, the rate-limiting enzyme in the synthesis of acetylcholine, also adopt several forms (Houser et al., 1983a), although with many common features similar to those found among the peptide neurons. Similarly, some cortical neurons immunoreactive for GAD, the enzyme involved in the synthesis of GABA, can also resemble the peptide neurons (Ribak, 1978; Hendrickson et al., 1981; Houser et al., 1983b). However, there is as yet no evidence for colocalization of a peptide with these markers for acetylcholine or GABA in cortical neurons.

Currently the best criteria for distinguishing morphological classes of intrinsic neuron in the cortex are axonal morphology (Jones, 1975) and sites of synaptic terminations (e.g., Fairén and Valverde, 1980). In the case of GABAergic cortical neurons (Ribak, 1978; Peters et al., 1982; Hendry et al., 1983a), different types can be detected on account of their individual patterns of synaptic organization. Comparison of synaptic sites indicates that both SRIF- and NPY-positive neurons of monkey cerebral cortex differ markedly from CCK-immunoreactive neurons of the cortex since the SRIF- and NPY-positive cells synapse mainly on small or medium-sized dendrites and on spines, and the CCK-positive cells synapse predominately on cell bodies and large proximal dendrites (Hendry et al., 1983b). Additional investigation will be necessary to determine whether similar distinctions can be used for further classifying peptide-immunoreactive neurons into subtypes, since this might have more functional significance than light microscopic morphology alone.

The significance of the selective laminar distribution of SRIF-positive and NPY-positive somata and the plexuses formed by their processes is uncertain. It is possible that this distribution is related in some way to the distribution of certain afferent fiber systems or to that of neurons receiving the synapses of these afferents. One plexus, and the cells mainly forming it, is in the supragranular layers where corticocortical afferents end (Jones et al., 1978, 1979). The deepest plexus in layer VI could have an association with cells at the center of one layer of thalamic afferent terminations and especially with cells projecting back to the thalamus (Lund et al., 1975; Gilbert and Kelly, 1975; Jones and Wise, 1977). In most areas a few cell bodies and varying numbers of processes immunoreactive for SRIF or NPY are also present among the thalamocortical terminations in the middle layers. This is particularly clear in the primary visual cortex, where dense plexuses of SRIF- and NPY-positive processes overlap one of the principal layers of thalamocortical fiber terminations in layer IVA and bracket that in layer IVC.

Previous immunocytochemical studies of the localization of GAD in cells and processes (Hendrickson et al., 1981; Fitzpatrick et al., 1983) and of the localization of serotonin (Kosofsky et al., 1983) in afferent axons have also revealed a rather strict laminar organization of immunoreactive processes in the monkey primary visual area. The distribution of the SRIF-positive and NPY-positive plexuses in the monkey visual cortex (Hendrickson, 1983; present study) resembles that of serotonin-positive fibers (Kosofsky et al., 1983) in being very dense just above and below layer IVC. Dopamine β-hydroxylase-containing fibers also end in relation to layer IV and other layers (Foote et al., 1983). The overlap of some transmitter-containing processes suggests the presence of combined effects of the various transmitters on cortical cells, but the nature of any differential effects that they exert, for example, on receptive field structure, has not been established.

Large numbers of SRIF- and NPY-positive cells are found in the subcortical white matter of monkeys. Preliminary findings indicate that the white matter cells in monkeys receive synapses on their proximal processes (S. H. C. Hendry and E. G. Jones, unpublished observations) and thus are probably neurons. These cells send radial processes into layers VI-IVCβ in monkey primary visual cortex and up to layers III and II in other areas of monkey cortex, where they contribute to the plexuses formed by the intracortical SRIF and NPY cells. It is not known whether these processes are axons or dendrites, although they look like the latter. Nor is the source of inputs to the white matter cells known. We observed no extremely large SRIF-positive cells in the subcortical white matter of monkeys such as those described in humans (Sorenson, 1982).

The difficulty of determining whether processes given off by SRIF- or NPY-immunoreactive cells are axons or dendrites is not restricted to cells in the white matter. Some of the branches given off by a single peptide-positive neuron in any layer of monkey cortex are of the appropriate size and morphology to be axons, but the larger processes can soon branch to form indentical processes. Virtually all appear beaded in the light microscope, and all beaded processes seen with the electron microscope contain numerous synaptic vesicles. It is possible,

therefore, that we are dealing with a class of cells without a conventional axon. In the electron microscope, synapses onto primary processes and proximal branches of the SRIF- and NPY-positive cells are evident (S. H. C. Hendry and E. G. Jones, unpublished observations), indicating that the processes probably function as dendrites. However, none of these processes has yet been followed for more than 40 μm from its parent soma, therefore, whether processes receiving synapses also give them off from their more distal beaded portions has not yet been satisfactorily determined.

Our electron microscopic findings reveal that three types of SRIF- and NPY-immunoreactive terminals are present in monkey cerebral cortex: (*1*) homogeneously labeled terminals forming symmetric synapses; (*2*) homogeneously labeled terminals forming no synaptic contacts; and (*3*) large terminals with only their large dense-core vesicles labeled, forming asymmetric synapses. It is likely that more extensive serial reconstructions of homogeneously labeled terminals will reveal most giving rise to symmetric synapses, although some terminals have been followed through series of sections and apparently do not synapse at any point.

The distribution of peptide immunoreactivity both in large dense-core vesicles and throughout the cytoplasm of terminals is common in the mammalian central nervous system (Pickel et al., 1977, 1980; Barber et al., 1979; Aronin et al., 1981; DiFiglia et al., 1982a, b; DiFiglia and Aronin, 1982), but the homogeneous labeling of terminals could conceivably result from the disruption of peptide-containing large dense-core vesicles during fixation or subsequent processing. Conversely, labeling of the large dense-core vesicles, particularly where this occurs in isolation, might also result during the tissue processing. The lack of labeling in large dense-core vesicles of most terminals in experimental material and in all terminals in control material suggests that our methods have not produced a general artifactual staining of all dense-core vesicles. Therefore, we tentatively conclude that there are two fundamentally distinct types of SRIF- and NPY-positive terminals, one with a mixed vesicle population and making symmetric or no synaptic contacts and a second with primarily dense-core vesicles and making asymmetric contacts.

Many of the symmetric synapses formed by SRIF- and NPY-positive terminals are on dendrites and spines, and the recipient cells therefore may be pyramidal or spiny nonpyramidal cells. Asymmetric synapses formed by the large SRIF- and NPY-labeled terminals occure on large dendrites covered with synapses. Similar dendrites have been identified previously in monkey precentral motor cortex as originating from large nonpyramidal cells of layers III to V (Sloper and Powell, 1979), and one dendrite receiving an asymmetric synapse from an NPY-positive terminal was traced to a large nonpyramidal cell of layer V. Neurons of similar size, dendritic morphology, and synaptic density in monkey SI and motor cortex were found to be GAD positive (Hendry et al., 1983a). These data are suggestive of synaptic relationships between the peptidergic neurons and several classes of other neurons in monkey cerebral cortex.

Whereas several studies have identified depolarizing or excitatory responses to SRIF application (Dodd and Kelly, 1978; Ioffe et al., 1978; Olpe et al., 1980; Phillis and Kirkpatrick, 1982), other studies have found SRIF to produce inhibitory or mixed effects in cortical (Renaud et al., 1975) and hippocampal (Pittman and Siggins, 1981) neurons and at subcortical sites (Chan-Palay et al., 1982; Renaud and Padjen, 1977). Rat cortical neurons in culture also exhibit mixed responses to SRIF application that are dependent upon the concentration of the peptide (Delfs and Dichter, 1983), with excitatory effects occurring at low concentrations and inhibitory effects occurring at higher concentrations. It is tempting to suggest that the excitatory and inhibitory effects of SRIF might occur through release at the different types of synapses that we have identified: asymmetric synapses in the case of excitation and symmetric synapses in the case of inhibition. However, the proportion of asymmetric synapses formed by SRIF-positive terminals appears very low, possibly too low to account for the predominantly excitatory effects of SRIF. In the cortex, symmetric synaptic contacts are also made by terminals immunoreactive for CCK, another putative excitatory peptide (Hendry et al., 1983b). It appears, therefore, that the traditional association of asymmetric synapses with excitatory effects and of symmetric synapses with inhibitory effects may not hold for peptide-releasing synapses in the cortex. In any case, only when physiological responses to SRIF release are determined at synapses examined ultrastructurally and the nature of transmitter-receptor interactions is identified at these synapses will it be clear whether the differences in response to SRIF are associated with differences in synaptic morphology.

In comparing SRIF-positive and NPY-positive neurons in rat and monkey cerebral cortex it is clear that a much greater proportion of cells in rats is immunoreactive for either peptide. We have also noted a similar difference in the proportion of rat and monkey cortical neurons immunoreactive for CCK (Hendry et al., 1983b). It is possible that the peptides are present in lower concentrations within neuronal somata in the monkey cortex, making it difficult to detect them immunocytochemically. However, attempts to increase the levels of SRIF and NPY in monkey cortex by injections of colchicine produced no increase in the number of immunocytochemically stained cells. It is also possible that a different molecular form of SRIF and NPY predominates in monkey cerebral cortex and that it is less well recognized by the antisera used. On the other hand, the results may reflect a genuine species difference in the populations of SRIF- and NPY-positive neurons, both in the cortex itself and in the subcortical white matter.

References

Allen, Y. S., J. E. Adrian, J. M. Allen, K. Tatemoto, T. J. Crow, S. R. Bloom, and J. M. Polak (1983) Neuropeptide Y distribution in the rat brain. Science *221:* 877–879.

Altschuler, R. A., M. Parakkal, W. G. Haser, R. J. Wenthold, and J. P. Donoghue (1983) Glutaminase and aspartate aminotransferase as markers for glutamergic/aspartatergic neurons in rodent and monkey cerebral cortex. Soc. Neurosci. Abstr. *9:* 261.

Aronin, N., M. DiFiglia, A. S. Liotta, and J. B. Martin (1981) Ultrastructural localization and biochemical features of immunoreactive Leu-enkephalin in monkey dorsal horn. J. Neurosci. *1:* 561–577.

Asanuma, H., and I. Rosén (1973) Spread of mono- and polysynaptic connections within cat's motor cortex. Exp. Brain Res. *16:* 507–520.

Barber, P. R., J. E. Vaughn, J. R. Slemmon, P. M. Salvaterra, E. Roberts, and S. E. Leeman (1979) The origin, distribution and synaptic relationships of substance P axons in rat spinal cord. J. Comp. Neurol *184:* 331–347.

Beinfeld, M. C., D. K. Meyer, R. L. Eskay, R. T. Jensen, and M. J. Brownstein (1981) The distribution of cholecystokinin immunoreactivity in the central nervous system of the rat as determined by radioimmunoassay. Brain Res. *212:* 51–57.

Bennett, G. W., J. A. Edwardson, D. Marcano de Cotte, M. Berelowitz, B. L. Pimstone, and S. Kronheim (1979) Release of somatostatin from rat brain synaptosomes. J. Neurochem. *32:* 1127–1130.

Bennett-Clarke, C., M. A. Romagnano, and S. A. Joseph (1980) Distribution of somatostatin in the rat brain: Telencephalon and diencephalon. Brain Res. *188:* 473–486.

Benoit, R., N. Ling, B. Alford, and R. Guillemin (1982) Seven peptides derived from pro-somatostatin in rat brain. Biochem. Biophys. Res. Commun. *107:* 944–950.

Brazeau, P., W. Vale, R. Burgus, N. Ling, M. Butcher, J. Rivier, and R. Guillemin (1973) Hypothalamic polypeptide that inhibits the secretion of immunoreactive pituitary growth hormone. Science *179:* 77–79.

Chan-Palay, V., M. Ito, P. Tongroach, M. Sakurai, and S. Palay (1982) Inhibitory effects of motilin, somatostatin, (Leu)enkephalin, (Met)

enkephalin and taurine on neurons of the lateral vestibular nucleus: Interactions with gamma-aminobutyric acid. Proc. Natl. Acad. Sci. U. S. A. *79:* 3355–3359.

Colonnier, M. L. (1966) The structural design of the neocortex. In *Brain and Conscious Experience*, C. Eccles, ed., pp. 1–23, Springer-Verlag, New York.

Delfs, J. R., and M. A. Dichter (1983) Effects of somatostatin on mammalian cortical neurons in culture: Physiological actions and unusual dose response characteristics. J. Neurosci. *3:* 1176–1188.

Dichter, M. A., and J.R. Delfs (1981) Somatostatin and cortical neurons in cell culture. In *Neurosecretion and Brain Peptides*, J. B. Martin, S. Reichlin, and K. L. Bick, eds., pp. 145–157, Raven Press, New York.

DiFiglia, M., and N. Aronin (1982) Ultrastructural features of immunoreactive somatostatin neurons in the rat caudate nucleus. J. Neurosci. *2:* 1267–1274.

DiFiglia, M., N. Aronin, and S. E. Leeman (1982a) Light microscopic and ultrastructural localization of immunoreactive substance P in the dorsal horn of monkey spinal cord. Neuroscience *7:* 1127–1139.

DiFiglia, M., N. Aronin, and J. B. Martin (1982b) Light and electron microscopic localization of immunoreactive Leu-enkephalin in the monkey basal ganglia. J. Neurosci. *2:* 303–320.

Dodd, J., and J. S. Kelly (1981) The actions of cholecystokinin and related peptides neurones of the mammalian hippocampus. Brain Res. *205:* 337–350.

Emson, P. C., and S. P. Hunt (1981) Anatomical chemistry of the cerebral cortex. In *The Organization of the Cerebral Cortex*, F. O. Schmitt, F. G. Worden, G. Adelman, and S. G. Daniels, eds., pp. 325–345, MIT Press, Cambridge, MA.

Emson, P. C., and S. P. Hunt (1984) Peptide containing neurones of the cerebral cortex. In *The Cerebral Cortex*, E. G. Jones and A. Peters, eds., Plenum Press, New York, in press.

Emson, P. C., and O. Lindvall (1979) Distribution of putative neurotransmitters in the neocortex. Neuroscience *4:* 1–30.

Emson, P. C., J. Fahrenkrug, and E. G. S. Spokes (1979) Vasoactive intestinal polypeptide (VIP) distribution in normal human brain and in Huntington's disease. Brain Res. *173:* 174–178.

Emson, P. C., S. P. Hunt, J. F. Rehfeld, N. Gotterman, and J. Fahrenkrug (1980) Cholecystokinin and vasoactive intestinal polypeptide in the mammalian CNS: Distribution and possible physiological roles. In *Neural Peptides and Neuronal Communication*, E. Costa and M. Trabucchi eds., pp. 63–74, Raven Press, New York.

Emson, P. C., M. R. Rossor, and C. M. Lee (1981) The regional distribution and chromatographic behavior of somatostatin in human brain. Neurosci. Lett. *22:* 319–324.

Fairén, A., and F. Valverde (1980) A specialized type of neuron in the visual cortex of the cat: A Golgi and electron microscopic study of chandelier cells. J. Comp. Neurol. *194:* 761–780.

Finley, J. C. W., J. L. Maderdrut, L. J. Roger, and P. Petrusz (1981) The immunocytochemical localization of somatostatin-containing neurons in the rat central nervous system. Neuroscience *6:* 2173–2191.

Fitzpatrick, D., J. S. Lund, and D. Schmechel (1983) Glutamic acid decarboxylase immunoreactive neurons and terminals in the visual cortex of monkey and cat. Soc. Neurosci. Abstr. *9:* 616.

Foote, S. L., J. H. Morrison, and F. E. Bloom (1983) Postnatal development of laminar innervation patterns by noradrengeric and serotoninergic fibers in monkey primary visual cortex. Soc. Neurosci. Abstr. *9:* 1150.

Fuxe, K., T. Hökfelt, S. I. Said, and V. Mutt (1977) Vasoactive intestinal polypeptide and the nervous system: Immunohistochemical evidence for localization in central and peripheral neurons, particularly intracortical neurons of the cerebral cortex. Neurosci. Lett. *5:* 241–246.

Gilbert, C. D., and J. P. Kelly (1975) The projection of cells in different layers of the cat's visual cortex. J. Comp. Neurol. *163:* 81–105.

Hendrickson, A. (1983) Pyramidal and stellate neurons in monkey visual cortex label for different peptides. Neurosci. Abstr. *9:* 821.

Hendrickson, A. E., S. P. Hunt, and J. -Y. Wu (1981) Immunocytochemical localization of glutamic acid decarboxylase in monkey striate cortex. Nature *292:* 605–607.

Hendry, S. H. C., C. R. Houser, E. G. Jones, and J. E. Vaughn (1983a) Synaptic organization of immunocytochemically identified GABA neurons in the monkey sensory-motor cortex. J. Neurocytol. *12:* 639–660.

Hendry, S. H. C., E. G. Jones, and M. C. Beinfeld (1983b) Cholecystokinin-immunoreactive neurons in rat and monkey cerebral cortex make symmetric synapses and have intimate associations with blood vessels. Proc. Natl. Acad. Sci. U. S. A. *80:* 2400–2404.

Hökfelt, T., O. Johansson, A. Ljungdahl, J. M. Lundberg, and M. Schultzberg (1980) Peptidergic neurones. Nature *284:* 515–521.

Hökfelt, T., J. M. Lundberg, L. Terenius, G. Jansco, and J. R. Kimmel (1981) Avian pancreatic polypeptide (APP) immunoreactive neurons in the spinal cord and spinal trigeminal nucleus. Peptides *2:* 81–87.

Hökfelt, T., M. Schultzberg, J. M. Lundberg, K. Fuxe, V. Mutt, J. Fahrenkrug, and S. I. Said (1982) Distribution of vasoactive intestinal polypeptide in the central and peripheral nervous systems as revealed by immunocytochemistry. In *Vasoactive Intestinal Peptide*, S. I. Said, ed., pp. 65–90, Raven Press, New York.

Houser, C. R., G. D. Crawford, P. M. Salvaterra, and J. E. Vaughn (1983a) Cholinergic neurons in rat cerebral cortex identified by immunocytochemical localization of choline acetyltransferase. Soc. Neurosci. Abstr. *9:* 80.

Houser, C. R., S. H. C. Hendry, E. G. Jones, and J. E. Vaughn (1983b) Morphological diversity of immunocytochemically identified GABA neurons in the monkey sensory-motor cortex. J. Neurocytol. *12:* 617–638.

Innis, R. B., F. M. A. Correa, G. R. Uhl, B. Schneider, and S. H. Snyder (1979) Cholecystokinin octapeptide immunoreactivity. Histochemical localization in rat brain. Proc. Natl. Acad. Sci. U. S. A. *76:* 521–525.

Ioffe, S., V. Havlicek, H. Friesen, and V. Chernick (1978) Effect of somatostatin (SRIF) and *l*-glutamate on neurons of the sensorimotor cortex in awake habituated rabbits. Brain Res. *153:* 414–418.

Iversen, L. L., S. D. Iversen, F. Bloom, C. Douglas, M. Brown, and W. Vale (1978) Calcium-dependent release of somatostatin and neurotensin from rat brain *in vitro*. Nature *273:* 161–163.

Jones, E. G. (1975) Varieties and distribution of non-pyramidal cells in the somatic sensory cortex of the squirrel monkey. J. Comp. Neurol. *160:* 205–268.

Jones, E. G. (1983) Identification and classification of intrinsic circuit elements in the neocortex. In *Dynamic Aspects of Neocortical Function*, G. Edelman, W. M. Cowan and W. E. Gall, eds., John Wiley & Sons, Inc., New York, in press.

Jones, E. G., and S. P. Wise (1977) Size, laminar and columnar distribution of efferent cells in the sensory-motor cortex of monkeys. J. Comp. Neurol. *175:* 391–438.

Jones, E. G., J. D. Coulter, and S. H. C. Hendry (1978) Intracortical connectivity of architectonic fields in the somatic sensory motor and parietal cortex of monkey. J. Comp. Neurol. *181:* 291–348.

Jones, E. G., J. D. Coulter, and S. P. Wise (1979) Commissural columns in the sensory-motor cortex of monkeys. J. Comp. Neurol. *188:* 113–136.

Kelly, J. S. (1982) Electrophysiology of peptides in the central nervous system. Br. Med. Bull. *38:* 283–290.

Kosofsky, B. E., M. E. Molliver, M. S. Lewis, and H. G. W. Lidov (1983) Tangential organization of the serotoninergic innervation of primate visual cortex. Soc. Neurosci. Abstr. *9:* 617.

Krisch, B. (1980) Differing immunoreactivities of somatostatin in the cortex and the hypothalamus of the rat. A light and electron microscopic study. Cell Tissue Res. *212:* 457–464.

Krnjević, K. (1974) Chemical nature of synaptic transmission in vertebrates. Physiol. Rev. *54:* 318–450.

Larsson, L. I., and J. E. Rehfeld (1979) Localization and molecular heterogeneity of cholecystokinin in the central and peripheral nervous system. Brain Res. *165:* 201–218.

Lechan, R. M., R. H. Goodman, M. Rosenblatt, S. Reichlin, and J. F. Habener (1983) Prosomatostatin-specific antigen in rat brain: Localization by immunocytochemical staining with an antiserum to a synthetic sequence of preprosomatostatin. Proc. Natl. Acad. Sci. U. S. A. *80:* 2780–2784.

Lorén, I., J. Alumets, R. Hokanson, and F. Sundler (1979) Distribution of gastrin and CCK-like peptides in rat brain. An immunocytochemical study. Histochemistry *59:* 249–257.

Lund, J. S. (1973) Organization of neurons in the visual cortex, area 17, of the monkey (*Macaca mulatta*). J. Comp. Neurol. *147:* 455–496.

Lund, J. S., R. D. Lund, A. E. Hendrickson, A. H. Bunt, and A. F. Fuchs (1975) The origin of efferent pathways from the primary visual cortex, area 17, of the macaque monkey as shown by retrograde transport of horseradish peroxidase. J. Comp. Neurol. *164:* 287–303.

Lundberg, J. M., T. Hökfelt, A. Anggåard, J. Kimmel, M. Goldstein, and K. Marley (1980) Coexistence of an avian pancreatic polypeptide (AP) immunoreactive substance and catecholamines in some peripheral and central neurons. Acta Physiol. Scand. *110:* 107–109.

McDonald, J. K., J. G. Parnavelas, A. N. Karamanlidis, and N. Brecha (1982a) The morphology and distribution of peptide-containing neurons in the adult and developing visual cortex of the rat. II. Vasoactive intestinal polypeptide. J. Neurocytol. *11:* 825–837.

McDonald, J. K., J. G. Parnavelas, A. Karamanlidis, and N. Brecha (1982b) The morphology and distribution of peptide-containing neurons in the adult and developing visual cortex of the rat. IV. Avian pancreatic polypeptide peptide. J. Neurocytol. *11:* 985–995.

McDonald, J. K., J. G. Parnavelas, A. Karamanlidis, N. Brecha, and J. I. Koenig (1982c) The morphology and distribution of peptide-containing neurons in the adult and developing visual cortex of the rat. I. Somatostatin. J. Neurocytol. *11:* 809–824.

McDonald, J. K., J. G. Parnavelas, A. K. Karamanlidis, N. Brecha, and G. Rosenquist (1982d) The morphology and distribution of peptide-containing neurons in the adult and developing visual cortex of the rat. III. Cholecystokinin. J. Neurocytol. *11:* 881–895.

Morrison, J. H., R. Benoit, P. J. Magistretti, and F. E. Bloom (1983) Immunohistochemical distribution of pro-somatostatin-related peptides in cerebral cortex. Brain Res. *262:* 344–351.

Nicoll, R. A. (1978) Peptide receptors in the CNS: Neurophysiologic studies in neurobiology of peptides. Neurosci. Res. Program Bull. *16:* 272–285.

Orpe, H.-R., V. L. Balcar, H. Bittiger, H. Rink, and P. Sieber (1980) Central actions of somatostatin. Eur. J. Pharmacol. *63:* 127–133.

Peters, A., and C. C. Proskauer (1980) Synaptic relationships between a multipolar stellate cell and a pyramidal neuron in the rat visual cortex. A combined Golgi-electron microscope study. J. Neurocytol. *9:* 163–183.

Peters, A., C. C. Proskauer, and C. E. Ribak (1982) Chandelier cells in rat visual cortex. J. Comp. Neurol. *206:* 397–416.

Peters, A., M. Miller, and L. M. Kimerer (1983) Cholecystokinin-like immunoreactive neurons in rat cerebral cortex. Neuroscience *8:* 431–448.

Phillis, J. W., and J. R. Kirkpatrick (1980) The actions of motilin, luteinizing hormone releasing hormone, cholecystokinin, somatostatin, vasoactive intestinal polypeptide and other peptides on rat cerebral cortical neurons. Can. J. Physiol. Pharmacol. *58:* 612–623.

Phillis, J. W., J. R. Kirkpatrick, and S. I. Said (1978) Vasoactive intestinal polypeptide excitation of central neurons. Can. J. Physiol. Pharmacol. *56:* 337–340.

Pickel, V. M., D. J. Reis, and S. E. Leeman (1977) Ultrastructural localization of substance P in neurons of rat spinal cord. Brain Res. *122:* 534–540.

Pickel, V. M., K. K. Sumai, S. C. Beady, R. J. Miller, and D. J. Reis (1980) Immunocytochemical localization of enkephalin in the neostriatum of rat brain: A light and electron microscopic study. J. Comp. Neurol. *189:* 721–740.

Pittman, Q. J., and G. R. Siggins (1981) Somatostatin hyperpolaries pyramidal cells *in vitro*. Brain Res. *221:* 402–408.

Ramón y Cajal, S. (1911) *Histologie du Système Nerveux de l'Homme et des Vertébrés*, Vol. 2, L. Azoulay, transl., Maloine, Paris.

Rehfeld, J. F. (1978) Immunochemical studies on cholecystokinin. II. Distribution and molecular heterogeneity in the central nervous system and small intestine of man and hog. J. Biol. Chem. *253:* 4022–4030.

Renaud, L. P., and A. Padjen (1977) Electrophysiological analysis of peptide actions in neural tissue. In *Centrally Acting Peptides*, J. Hughes, ed., pp. 59–84, MacMillan, New York.

Renaud, L. P., J. B. Martin, and P. Brazeau (1975) Depressant action of TRH, LH-RH and somatostatin an activity of central neurons. Nature *255:* 233–235.

Ribak, C. E. (1978) Aspinous and sparsely-spinous stellate neurons in the visual cortex of rats contain glutamic acid decarboxylase. J. Neurocytol. *7:* 461–478.

Sims, K. B., D. L. Hoffman, S. I. Said, and E. A. Zimmerman (1980)Vasoactive intestinal polypeptide (VIP) in mouse and rat brain: An immunocytochemical study. Brain Res. *186:* 165–183.

Sloper, J. J., and T. P. S. Powell (1979) Ultrastructural features of the sensori-motor cortex of the primate. Philos. Trans. R. Soc. Lond. Biol. *285:* 123–138.

Somogyi, P. (1977) A specific axo-axonal interneuron in the visual cortex of the rat. Brain Res. *136:* 345–350.

Somogyi, P., and A. Cowey (1981) Combined Golgi and electron microscopic study on the synapses formed by double bouquet cells in the visual cortex of the cat and monkey. J. Comp. Neurol. *195:* 547–566.

Sorenson, K. V. (1982) Somatostatin: Localization and distribution in the cortex and the subcortical white matter of human brain. Neuroscience *5:* 1227–1232.

Srikant, C. B., and Y. C. Patel (1981) Somatostatin receptors: Identification and characterization in rat brain membranes. Proc. Natl. Acad. Sci. U. S. A. *78:* 3930–3934.

Straus, E., and R. S. Yalow (1978) Species specificity of cholecystokinin in gut and brain of several mammalian species. Proc. Natl. Acad. Sci. U. S. A. *75:* 486–489.

Szentágothai, J., and M. Arbib (1974) Conceptual models of neural organization. Neurosci. Res. Program Bull. *12:* 307–510.

Tatemoto, K., M. Carlquist, and V. Mutt (1982) Neuropeptide Y—A novel brain peptide with structural similarities to peptide YY and pancreatic polypeptide. Nature *296:* 659–660.

Toyama, K., M. Kimura, and K. Tanaka (1981) Organization of cat visual cortex as investigated by cross-correlation technique. J. Neurophysiol. *46:* 202–214.

Valverde, F. (1971). Short axon neuronal subsystems in the visual cortex of the monkey. Int. J. Neurosci. *1:* 181–197.

Vincent, S. R., O. Johansson, T. Hökfelt, B. Meyerson, C. Sachs, R. P. Elde, L. Terenius, and J. Kimmel (1982a) Neuropeptide coexistence in human cortical neurones. Nature *298:* 65–67.

Vincent, S. R., L. Skirboll, T. Hökfelt, O. Johansson, J. M. Lundberg, R. P. Elde, L. Terenius, and J. Kimmel (1982b) Coexistence of somatostatin- and avian pancreatic polypeptide (APP)-like immunoreactivity in some forebrain neurons. Neuroscience *7:* 439–446.